ADDIS ABABA UNIVERSITY

COLLEGE OF TECHNOLOGY AND BUILT ENVIROMENT

SCHOOL OF ELECTRICAL AND COMPUTER ENGINEERING

COMMUNICATION ENGINEERING GRADUATE PROGRAM

Thesis On

MICROSTRIP FED BANDWIDTH ENHANCEMENT OF A MM WAVE PIFA ANTENNA FOR 5G MOBILE COMMUNICATION

A thesis submitted to the School of Electrical and Computer Engineering in Partial Fulfillment of the requirements for the Degree of Masters of Science in Communication Engineering

By

Elias Ayana Gezu

Advisor

Murad Ridwan (PhD)

February 26 2026 E.C

Addis Ababa, Ethiopia

ADDIS ABABA UNIVERSITY

COLLEGE OF TECHNOLOGY AND BUILT ENVIROMENT

SCHOOL OF ELECTRICAL AND COMPUTER ENGINEERING

MICROSTRIP FED BANDWIDTH ENHANCEMENT OF A MILLIMETER WAVE PIFA ANTENNA FOR 5G MOBILE COMMUNICATION

By: ELIAS AYANA

Approved by Board of Examiners

Chair Person	Signature
Dr. Murad Ridwan	
Adviser	Signature
Internal Examiner	Signature
External Examiner	Signature

Declaration

I, the undersigned, hereby declare that the research paper entitled "Microstrip-Fed Bandwidth Enhancement of a mm-Wave PIFA Antenna for 5G Mobile Communication is my own work in compliance with internationally accepted practices; I fully acknowledge and refer all materials used in this thesis work.

Elias Ayana _____

Name Signature

Place: Addis Ababa University, Ethiopia

Date of Submission: Nov. 15 2025

This thesis has been submitted for examination with my approval as a university advisor.

Dr. Murad Ridwan _____

Adviser Signature

Acknowledgment

First and foremost, I thank Almighty God and His blessed mother, Saint Mary, for their divine guidance and countless blessings throughout my life and studies.

I would like to express my deepest gratitude to my advisor, **Dr. Murad Ridwan**, for his invaluable guidance, encouragement, and continuous support throughout this research. His professional insight and constructive feedback have been essential to the success of this work.

I also thank the **School of Electrical and Computer Engineering, the Department of Communication Engineering of Addis Ababa University**, and all of my teachers for their guidance and academic support.

My heartfelt thanks go to my family and friends for their prayers, motivation, and moral support throughout my academic pursuit.

Finally, My sincere appreciation also goes to my beloved wife, **Mrs. Nardos Belay** , for her unwavering support, patience, and encouragement during this journey.

Abstract

With the rapid evolution of 5G mobile communication, achieving wideband performance in millimeter-wave (mmWave) antennas has become critical for ensuring high data rates and reliable connectivity. This research investigates bandwidth (BW) enhancement techniques for a 28 GHz planar inverted-F antenna (PIFA) designed for 5G smartphone applications. The conventional PIFA exhibits limited impedance bandwidth and moderate radiation performance, with a VSWR of 1.8, gain of 3.37 dB, and radiation efficiency of 74.7%. To overcome these limitations, several BW enhancement methods—including height (h) improvement, width (W_s) optimization, slot loading, defected ground structure (DGS) implementation, and parasitic element integration—are systematically evaluated. Simulation results demonstrate that structural modifications such as slot loading and DGS significantly broaden the impedance bandwidth up to 841 MHz, compared to the conventional PIFA, while maintaining acceptable radiation efficiency (61–64.5%) and gain (2.69–3.54 dB). The DGS and parasitic techniques achieve the lowest VSWR (≈1.07–1.11), improved angular beamwidth, and stable main lobe directions, indicating enhanced radiation characteristics suitable for 5G mobile devices. Parametric analyses reveal that subtle geometric adjustments, including substrate height and patch width tuning, can further optimize the antenna's impedance matching and radiation performance. The comparative study confirms that the proposed BW enhancement strategies effectively extend the operational bandwidth by up to 14.3% while maintaining satisfactory gain and efficiency, making them promising candidates for compact mmWave PIFA designs in 5G mobile communication systems. These findings provide valuable guidelines for designing high-performance wideband mmWave antennas, balancing impedance bandwidth, radiation efficiency, and gain for next-generation mobile applications.

KEY WORDS: PIFA, DGS, EBG, AMC, 5G, SLOTLOADING, BW

Contents

List of Figures

List of Acronyms

AMC	Artificial Magnetic Conductor
BW	Band Width
CST	Computer Simulating Tool
DGS	Deffective Ground Structure
EBG	Electromagnetic Bandgap
EM	Electro Magnatic
GA	Genetic Algorithm
GHz	Giga Hertz
IR	Infrard Radiation
IR	Infrard Radiation
mm	millimeter
PIFA	Planner Inverted F-Antenna
SAR	Specfic Absorption Rate
TM	Transvers Magnetic
VSWR	variable Standing Wave Radio
5G	Fifth Generation
RLSA	Radial line slot array antenna

Chapter 1

Introduction

1.1 Background

The Planar Inverted F Antenna (PIFA) is a compact, planar antenna design widely adopted in the wireless industry. The PIFA antenna has several advantages, such as low profile, ease of integration, and good radiation characteristics. These attributes make PIFA antennas suitable for mobile devices where space and design constraints are extremely important. Millimeter (mm-wave) frequencies, ranging from 30 to 300 GHz, have become a promising solution to meet these requirements. Among the various components that support 5G networks, millimeter-wave PIFA antennas play a vital role in supporting efficient communications. In the context of 5G, millimeter-wave PIFA antennas are designed to operate in the high frequency range, typically around 28 to 39 GHz. These antennas use the concept of the PIFA structure but are optimized for these specific frequency bands. Millimeter wave PIFA antennas are designed to support higher data rates, wider bandwidth, and improved overall performance compared to lower frequency antennas. In the realm of 5G, which promises ultra-fast speeds and low latency, the need for efficient and effective antennas is critical. Millimeter wave PIFA antennas are commonly used because of their compact size, ease of integration, and radiation pattern characteristics. However, it often faces challenges with limited bandwidth, which can hinder its ability to transmit and receive large amounts of data at these higher frequencies. its inherently narrow bandwidth limits its application in broadband 5G systems. Several techniques have been employed to enhance the bandwidth of mmWave PIFA antennas. Increasing the antenna height reduces the quality factor by

lowering stored reactive energy, resulting in improved impedance bandwidth [1]. Widening the shorting strip decreases inductive reactance and stabilizes impedance matching over a wider frequency range [2]. Slot loading on the radiating patch alters current paths and introduces multiple resonant modes that combine to enhance bandwidth [3]. The addition of parasitic elements enables electromagnetic coupling that generates additional resonances, further extending the operational bandwidth [4]. Moreover, the implementation of defected ground structures (DGS) disturbs ground current distribution and suppresses surface waves, leading to significant bandwidth improvement and better radiation performance in compact mmWave PIFA designs [5]

1.2 Statement of the Problem

The rapid deployment of fifth-generation (5G) mobile communication systems has created a strong demand for compact, low-profile antennas capable of operating efficiently in millimeter-wave (mmWave) frequency bands. Planar Inverted-F Antennas (PIFAs) are widely favored for mobile devices due to their compact size, ease of integration, and specific particular absorption rate (SAR). However, conventional mmWave PIFA antennas inherently suffer from narrow impedance bandwidth, which limits their ability to support wideband 5G applications and reduces overall system reliability under fabrication tolerances and user-hand effects. Achieving a wide bandwidth in mmWave PIFA antennas is particularly challenging due to strict size constraints in smartphones and the high sensitivity of antenna performance to geometrical variations at high frequencies. Techniques such as increasing antenna height, enlarging the radiating patch width, introducing slot loading, adding parasitic elements, and incorporating defected ground structures (DGS) have individually shown potential for bandwidth enhancement. Therefore, the problem addressed in this research is to systematically investigate and optimize these structural modifications to enhance the impedance bandwidth of a mmWave PIFA antenna for 5G mobile communication, while maintaining compact size, stable radiation characteristics, and suitability for smartphone integration.

1.3 Objective

1.3.1 General Objective

To enhance the bandwidth of a millimeter-wave planer inverted F- Antenna(PIFA) for 5G mobile communication.

1.3.2 Specific Objective

- To Study the limitations of existing MM wave PIFA antennas in terms of bandwidth
- Explore different techniques to improve the bandwidth performance of antennas
- Design and simulation of a conventional MM wave PIFA antenna using microstrip feeding.
- To enhance the BW using the slot loading technique
- To Use Parasitic Elements to enhance the bandwidth
- To enhance the BW using DGS techniques
- To increase the height and width of the shorthning plate of the Antenna to enhance the bandwidth.
- To Compare the performance of the Antenna through different techniques in terms of bandwidth improvement.
- Provide recommendations and information to further enhance the bandwidth of MM wave PIFA antennas for 5G mobile communications.

1.4 Methodology

The bandwidth of the PIFA mmWave antennas will be enhanced for 5G mobile communications using diffrent structural techniques.

Review and research of the literature: A review of research and research papers on PIFA bandwidth enhancement and 5G Mobile Communications. Learn the advanced techniques and methods.

Design and simulation of antennas: Determine the appropriate operating frequency range for 5G mm Wave communications and design the PIFA antenna structure considering size, material selection, and desired performance parameters.

coaxial Proximity feeding Understanding of the coaxial proximity feed. Define the dimensions and distance between the coaxial probe and the PIFA antenna structure.

Slot Loading : Slot loading enhances the bandwidth of a mmWave PIFA antenna by introducing additional resonant modes and improving impedance matching. **Defective Ground plane Structure (DGS)** A DGS enhances the bandwidth of a mmWave PIFA antenna by introducing slots or patterns in the ground plane, which disturb the current distribution and create additional resonances. This technique reduces surface wave losses and improves impedance matching over a wider frequency range.

parameter optimization: Widening the shorting plate diminishes the quality factor of the antenna by improving the current distribution and aligning impedance, while reducing the thickness of the antenna results in a decrease in reactive energy storage.

Comparison and optimization: Compare and evaluate the results of each technique. Identify the most effective bandwidth improvement techniques for the PIFA antenna.

Documentation and reporting: Synthesize findings, methods, and recommendations into a comprehensive report or thesis. Present the results through technical documentation, diagrams, and visual aid.

1.5 Outline of the thesis

Chapter 1, Introduction

- Background of 5G Mobile Communications and Millimeter Wave PIFA Antennas.
- The Importance of Bandwidth Enhancement for Effective 5G Communications.

Chapter 2,Literature Review

- Analyze the limitations and challenges faced in achieving a broad bandwidth.
- Review of recent studies on improving bandwidth of PIFA Antenna

Chapter 3, Design and methods

- Detailed description of the millimeter wave PIFA antenna .
- Explanation of microstrip feeding (coaxial feeding), Slot loading and parasite addition, DGS techniques,increasing width of the shorthning plate and reducing the thickness of the substrate material.
- Theoretical and mathematical analysis of each technique.
- Configuration parameters and simulation.

Chapter 4, Results and analysis

- Presentation and discussion of simulation results for each technique.
- Evaluation of the bandwidth improvement achieved with.
- Comparison of results with conventional antenna types.

Chapter 5, Conclusions

- Summary of research results.
- Key contributions to the field of millimeter-wave PIFA antennas for 5G.
- Implications and potential future directions for bandwidth enhancement research.

References

- List of documents cited and documents used in the thesis.

Chapter 2

Literature Review

The rapid adoption of 5G mobile communication has stimulated significant research on millimeter wave (mm Wave) antennas, One of the main challenges is the limited bandwidth of millimeter Wave PIFAs. Researchers have explored advanced techniques to enhance it. In [6] demonstrated a metamaterial-loaded PIFA that achieved a bandwidth improvement of more than 30%over conventional designs. Similarly, in. [7] reported the use of ceramic substrates with a high dielectric constant, which allows for a compact design while maintaining wide bandwidth characteristics. These studies highlight that the integration of new materials not only expands the operating bandwidth but also improves the efficiency and gain of the antenna. [8] used slit designs to achieve multi-resonant characteristics, effectively expanding the usable bandwidth. Another innovative approach was presented by [9] who integrated stacked radiating elements to support multiple resonant frequencies, allowing 40% to improve the bandwidth. Furthermore, it has been shown that the implementation of folded PIFA structures allows the optimization of the antenna volume while increasing its bandwidth. The experimental results show that PIFA performs well with a $-10dB$ impedance bandwidth of 14.5% (3.17 to 3.67 GHz). The antenna must be suitable for 5G front end applications [10]. To improve the bandwidth, a flat planar inverted-F antenna (PIFA) with TM 0.1/2 and TM 2.1/2 modes in a single patch resonator is proposed. A pair of shorted pins is appropriately loaded under the laterally shorted radiation patch to study the variation of their resonant frequencies in the odd mode. The results show that the resonance frequency of the TM 0.1/2 mode (f 0.1/2) increases dramatically, while that of the TM 2.1/2 mode (f 2.1/2) is almost maintained. Thereafter, the width of the radiation spot is gradually

increased to bring f 2.1/2 closer to f 0.1/2.Using this approach, the dual radiation resonance modes can be remapped close to each other. Then, the proposed antenna, which resulted in an impedance bandwidth of about 15.3%, was significantly expanded by the advent of two in-band attenuation poles. [11]. In [12] the bandwidth were enhanced by studying the effect of varying the width of the input plate or feeding and shortening the plate on the impedance bandwidth. PIFA has been shown to have a bandwidth of up to 65%. In [13] propose a reconfigurable microstrip-fed PIFA for millimeter-wave 5G applications to solve the narrow bandwidth problem. The antenna uses two independently controlled parasitic elements, allowing the antenna impedance to be adjusted over a wide frequency range. This method achieves an improvement of approximately 33% bandwidth while maintaining a compact antenna size suitable for integration into mobile devices.In [14] propose a bandwidth enhancement technique using dual-band PIFA microstrip feed antennas for 5G base stations. By integrating dual resonators into the design, the antenna achieves a 29.8% and 30.4% wider impedance bandwidth in the lower and higher frequency bands of 5G, respectively. The proposed design achieves a compact form factor while maintaining excellent radiation characteristics.In [15], a highly miniaturized arc-shaped antenna structure operating at 28 GHz was introduced for potential millimeter-wave applications in the 5G frequency band. The circular monopole antenna has a radius of 1.3 mm. An elliptical slot integrated into the radiating surface contributes to achieving an improved bandwidth, resonating at the designated frequency of 28 GHz. The inclusion of this elliptical slot facilitates the creation of additional resonance, thus enhancing the bandwidth. With ultra-compact dimensions of 5 $\times$ 3 $\times$ 1.6 mm3, The designed antenna offers an impedance bandwidth of 15.73% (ranging from 25.83 to 30.24 GHz). In [16], the development of a 5G dual-band PIFA antenna, made from a cost-effective substrate, is discussed. It aims for a small size and wide bandwidth at frequencies of 28 GHz and 38 GHz. The antenna has a shorted patch and a modified U-shaped slot, providing good impedance matching and a clean radiation pattern. It offers bandwidths of 3.34 GHz and 1.395 GHz.

In [17], the article studies an adaptable and portable microstrip antenna intended for Sub-6 GHz 5G applications. It has a unique ground structure and is constructed of low-loss material, resulting in a peak gain of around 5. 57 dBi at a frequency of 2. 185 GHz and a reflection coefficient of -22.34 dB. At a certain distance, the lowest SAR value is 0. 0959 W/kg for 1 g and 0. 0755 W/kg for 10 g of tissue. In [18], Researchers have investigated strategies

to increase the bandwidth of microstrip antennas operating at microwave frequencies. The mm-wave band has several drawbacks, including restricted coverage and significant link losses. The study compares the performance of various wideband 5G antennas and examines several methods to increase bandwidth. In [19], At 28 GHz, in this study, the electromagnetic band gap (EBG) and the artificial magnetic conductor (AMC) are examined in a radial line slot array antenna (RLSA). The antenna performance is enhanced by the addition of EBG and AMC structures, which results in a low S11 value of -41. 4686 dB at 29. 86 GHz, a directivity of 25. 60 dBi, and a gain of 25. 26 dB at 28 GHz. This antenna is ideal for use in satellite communication and RADAR systems because the AMC lowers side lobes and improves directivity to 26. 10 dBi.

studies published In [20]indicate that the impedance bandwidth remains relatively limited or that the solutions are not feasible for practical application. They illustrated that various shaped feed plates can enhance impedance bandwidth, achieving up to approximately 25% fractional bandwidth, but did not analyze the dimensions of the feed plate and used a significantly large shortening plate. In [21] one examines how the variation of both the feed width and the width of the shorting plate influences the impedance bandwidth of the antenna. And also it will find the impacts of the slot loading, the DGS and the parasitic methods over enhancing the bandwidth of the mm wave PIFA antenna. The findings reveal that considerably wider bandwidth.

2.1 Mobile Antennas

MmWave single-element mobile antennas are compact antennas designed for high-frequency 24–40 GHz 5G bands. They prioritize miniaturization, wide bandwidth, and integration into smartphones or wearable devices.Common types include .

2.1.1 Planar Inverted-F Antenna (PIFA)

A PIFA is a compact, low-profile antenna consisting of a radiating plate, shorting pin, feed pin, and ground plane. At mmWave frequencies, PIFAs are widely used in smartphones due to their small footprint and good impedance matching. Bandwidth is naturally narrow but can be enhanced using slots, parasitic elements, or defected ground structures (DGS). PIFAs are relatively robust against hand effects and metal frames, making them ideal for

edge-mounted mobile antennas.

2.1.2 Microstrip Patch Antenna

A microstrip patch antenna consists of a metallic patch printed on a dielectric substrate over a ground plane. At mmWave frequencies, patches become electrically small, enabling compact integration. They provide stable radiation patterns and are easy to model and fabricate. However, they suffer from narrow bandwidth and high sensitivity to user proximity. In smartphones, patch antennas are mostly used as single elements within phased arrays or antenna-in-package (AiP) solutions.

2.1.3 Slot Antenna

Slot antennas radiate through a narrow opening etched in a ground plane or metal frame. At mmWave frequencies, they offer wider bandwidth than patches and excellent integration with metal-rim smartphones. Slot antennas are less sensitive to hand blockage and can be fed using microstrip or CPW lines. Variants such as U-slots or L-slots are common in 28 GHz and 39 GHz mobile devices, especially for side-edge implementations.

2.1.4 Monopole Antenna (Printed / Folded)

A printed monopole antenna is a quarter-wavelength radiator printed on a substrate and referenced to a ground plane. At mmWave frequencies, monopoles are very compact and easy to feed but strongly affected by ground size and user interaction. Efficiency degradation and impedance instability are common challenges. Folded or meandered versions are sometimes used in mobile devices, though monopoles are more popular at sub-6 GHz than mmWave.

2.1.5 Loop Antenna

Loop antennas operate based on magnetic field radiation and typically occupy a compact closed-loop structure. At mmWave frequencies, loop antennas offer stable impedance and reduced sensitivity to user hands compared to monopoles. However, their radiation resistance is low, resulting in limited gain and bandwidth. In smartphones, loop antennas are sometimes used as auxiliary or diversity elements rather than primary mmWave radiators.

2.1.6 Dielectric Resonator Antenna (DRA)

A DRA uses a high-permittivity dielectric block to radiate electromagnetic energy without metal conductors. At mmWave frequencies, DRAs provide high radiation efficiency, wide bandwidth, and low loss. They are well suited for 28 GHz and 39 GHz applications but require additional height and precise fabrication. Due to packaging constraints, DRAs are more common in research prototypes or mmWave modules than in ultra-thin smartphones.

2.1.7 Vivaldi (Tapered Slot) Antenna

The Vivaldi antenna is a traveling-wave tapered slot antenna known for ultra-wideband performance and stable radiation patterns. At mmWave frequencies, it offers high gain and broad bandwidth but requires a relatively large physical aperture. This limits its use in smartphones. Vivaldi antennas are more commonly found in mmWave measurement systems, radar, or external modules rather than directly integrated mobile handsets.

2.1.8 Antenna-in-Package (AiP)

Antenna-in-Package (AiP) integrates the antenna directly inside the RF package along with the transceiver. At mmWave frequencies, this approach minimizes feed loss, improves efficiency, and enables compact phased-array solutions. Single-element AiP antennas are often patch or slot-based. AiP is a key enabling technology for 5G mmWave smartphones, especially at 28 GHz and 39 GHz.

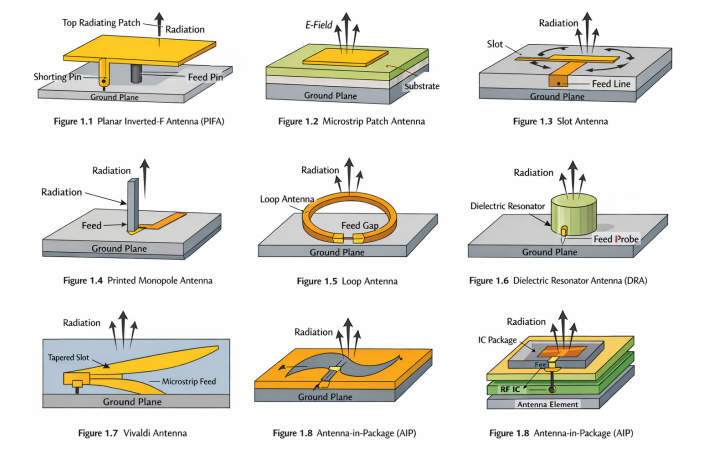

Figure 2.1: mobile Antenna types [22]

2.1.9 Why PIFA

For mmWave single-element mobile antennas PIFA stands out for 5G mobile applications. It offers a low-profile, compact, and planar structure, making it ideal for modern smartphones where space is limited. Its broadside radiation pattern efficiently directs energy toward the user while reducing backward radiation, minimizing SAR. It also provides good impedance bandwidth and ease of integration with other components, especially when combined with Defected Ground Structures (DGS) to enhance performance at mmWave frequencies like 28 GHz. Unlike traditional patch antennas, PIFA's vertical shorting pin allows size reduction without significant efficiency loss. Its robust performance in proximity to the hand or head makes it reliable for mobile use. Overall, the PIFA balances compactness, bandwidth, efficiency, and user safety, making it a top choice for single-element 5G mobile antennas.

2.2 Antenna Theory and Parameters

2.2.1 Antenna Theory

The antenna is a specialized transducer that converts electric current into electromagnetic (EM) waves or vise versa. Antennas are used to transmit and receive non-ionizing EM fields, including radio waves, microwaves, infrared radiation (IR), and visible light. Antennas are often classified as transmitting or receiving. However, many antennas can do both through the transceiver.

2.2.2 Antenna Parameters

Antenna parameters are used to describe the performance of an antenna when designing and measuring antennas.

2.2.3 Radiation Pattern

The radiation pattern is expressed as the relative power of a radiated field in different directions of an antenna. It is characterized as "the spatial distribution of a quantity that characterizes the electromagnetic field generated by the antenna". A two dimensional pattern can be a function of the elevation angle, θ, at constant azimuth angle, ϕ, or a function of ϕ at constant θ value [23]. The spherical coordinate system is shown in Figure 2.1. The

antenna radiation fields can be divided into three regions, a reactive near-field, radiating near-field, and far-field. A short distance away from the reactive near-field, the radiating near-field becomes dominant, and it is the region where the radiation field of an antenna is taking its form. The field pattern at the large distances refers to the term far field. The far field is the radiated power, also called the radiation field, and is what is most commonly of interest. Usually, measurements and beam patterns are observed in the far-field region, since this eases the calculations [22].

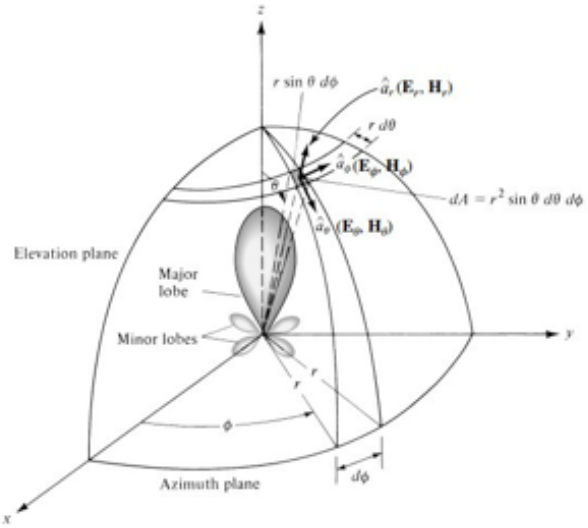

Figure 2.2: Spherical Coordinate Systems for Antenna Analysis [22]

2.2.4 Directivity

The directivity of an antenna has been defined as "the ratio of the intensity of the radiation in the direction provided by the antenna to the intensity of the radiation averaged in all directions". Where the average radiation intensity, U0, is equivalent to the total power radiated by the antenna divided by 4π, which is the radiation intensity of an isotropic source. This can be expressed as follows.

$$D(\theta, \phi) = \frac{U(\theta, \phi)}{U_0} = 4\pi \frac{U(\theta, \phi)}{P_{rad}} \tag{2.1}$$

Where,D is the directivity of the antenna U is the radiation intensity of the antenna U_0 is the radiation intensity of an isotropic source P_{rad} is the total power radiated.

2.2.5 Gain

The gain is defined as "the ratio of the intensity, in a given direction, to the radiation intensity that would be obtained if the power accepted by the antenna were transmitted isotropically" [24]. The relationship between antenna gain and directivity can be expressed by equation 2.2:

$$G(\theta, \phi) = 4\pi \frac{U(\theta, \phi)}{P_{in}} = 4\pi\eta \frac{U(\theta, \phi)}{P_{rad}} = \eta D(\theta, \phi) \tag{2.2}$$

where G is the gain of the antenna and D is the directivity of the antenna. P_{in} = total input power [W] η = antenna efficiency ($0 < \eta < 1$)

2.2.6 Antenna Efficiency

The reflection efficiency is related to the mismatch produced between the feeding line and the antenna when their impedance is different. The conduction efficiency is the ratio between the input power and the losses produced in the conductors of the antenna, and the same applies to the dielectric efficiency, but taking into account the losses in the dielectric of the antenna instead of its conductors. Then, the total efficiency of an antenna is defined as follows,

$$e_0 = e_r e_c e_d \tag{2.3}$$

Where, e_0 = total efficiency e_r = reflection efficiency (mismatch) e_c = conduction efficiency e_d = dielectric efficiency. The radiation efficiency of the antenna is a multiplication of the conduction efficiency and the dielectric efficiency. The loss is due to: conduction and dielectric, this is called the I^2R losses.

2.2.7 Input Impedance

The input impedance of an antenna is characterized by [22] "the impedance presented by an antenna at its terminals or the proportion of voltage to current at both terminals or the proportion of the proper components of the electric to magnetic fields at a point". These two impedance's see each other as similar, and it minimizes the reflection. Hence, the impedance of the antenna can be written as in equation 2.4.

$$Z_{in} = R_{in} + X_{in} \tag{2.4}$$

Where, Z_{in} is the impedance of the antenna R_{in} is the resistance of the antenna,X_{in} is the antenna reactance.

The imaginary part,X_{in} of the input impedance that represents the power stored in the near field of the antenna. The resistive part R_{in} of the input impedance comprises two components, radiation resistance R_r and loss resistance R_L. The power associated with the radiation resistance is the power actually radiated by the antenna, while the power dissipated in the loss resistance is lost as heat in the antenna itself due to dielectric or conducting losses[22]. Impedance matching to minimize reflections is achieved by making the input impedance equal to the source impedance as given in equation 2.5.

$$Z_{in} = Z_s^* \tag{2.5}$$

Where $Z_{in} = R_{in} + jX_{in}$ $Z_s = R_s + jX_s$ Z_s is the source impedance R_s is the source resistance X_s is the source reactance. The maximum power transfer occurs when Z_{in} is the complex conjugate of Z_s. In other words, $R_{in} = R_s$ and X_{in} = -X_s. If the condition for matching is not satisfied, then some of the power maybe reflected back, preventing all the power from reaching the destination point, and this prompts to the creation of standing waves, which can be described by a parameter called the Voltage Standing Wave Ratio (VSWR).

2.2.8 VSWR

VSWR is a ""reflection coefficient" function" which is a measure of the reflected power from the antenna. When the reflection coefficient Γ is given, the value of VSWR is calculated using equation 2.6 [25]:

$$VSWR = \frac{1+\Gamma}{1-\Gamma} \tag{2.6}$$

$$\Gamma = \frac{V_r}{V_i} = \frac{Z_{in} - z_s}{Z_{in} + z_s} \tag{2.7}$$

Where, Γ is called the reflection coefficient V_r is the amplitude of the reflected wave V_i is the amplitude of the incident wave.

The VSWR is basically a measure of the impedance mismatch between the transmitter and the antenna. The minimum VSWR is one, this represents a perfect match. In that situation,

the power is not reflected from the antenna, which is ideal. Equation 2.9 shows that the antenna with a lower VSWR, compared to the other antenna having a higher VSWR, has a better return loss. A practical antenna design should have an input impedance of 50 Ω or 75 Ω since most radio equipment is built for this impedance.

2.2.9 Return Loss

It is a parameter that is used to measure the power reflected by the antenna due to the mismatch between the transmission line and antenna. Thus, the return loss is a parameter like the VSWR to demonstrate how well the matching between the transmitter and receiver has occurred. Its measurement describes the ratio of the reflected power in the reflected wave to the power in the incident wave in units of decibels [[22] – [26]]. The Return Loss is given by:

$$\text{ReturnLoss} = -20 \log |\Gamma| \, (\text{dB}) \tag{2.8}$$

Here $|\Gamma|$ represents the magnitude of the reflection coefficient and this value is always below 1. For ideal matching between the transmitter and the receiver, $\Gamma = 0$ and $R_L = -\infty$ which implies that no power would be reflected back, where as a $\Gamma = 1$ has a $R_L = 0dB$, which implies that the antenna does not radiate anything because the power provided to the antenna is completely reflected. The Return Loss can also be calculated from the VSWR using equation 2.9. Note that the return loss is given as a ratio expressed in decibels.

$$\text{ReturnLoss} = -20 \log \frac{VWSR - 1}{VWSR + 1}, \text{dB} \tag{2.9}$$

Return loss is given as a negative figure. Being a loss, the returned power must be less than the forward power, and hence the return loss has a minus sign, or negative figures of decibels represent a loss.

2.2.10 S-parameters

The S-parameters are very important in microwave design for describing the behavior of electrical devices. Most of the electrical properties, i.e. VSWR, return loss, gain, etc., are

related to the S parameters. The S-parameters characterize the input and output relationship between ports in an electrical system. The S-parameters S11 and S22 represent the reflection of the input and output, while S21 is the forward transmission coefficient (gain) and S12 is the reverse transmission coefficient (isolation), which measures the power transferred from port 1 to port 2 [27].

The bandwidth of an antenna is defined as the range of frequencies over which the performance of the antenna. The bandwidth is the difference between the highest frequency (F_H) and the lowest frequency (F_L) for a particular band, as shown in equation 2.10.

$$B_W = F_H - F_L \tag{2.10}$$

The bandwidth can also be described in terms of percentage of the center frequency of the band as:

$$B_W = 100 \times \frac{F_H - F_L}{F_c} \tag{2.11}$$

Where, F_H is the highest frequency, F_L is the lowest frequency, and F_C is the center frequency in the band.

2.3 PIFA Antenna

The Planar Inverted-F (PIFA) antenna is increasingly used in the mobile phone market. The antenna is resonant at a quarter-wavelength (thus reducing the required space needed on the phone) and also typically has good SAR properties. This antenna resembles an inverted F, which explains the name PIFA. The PIFA is shown from a side view in Figure 2.5.

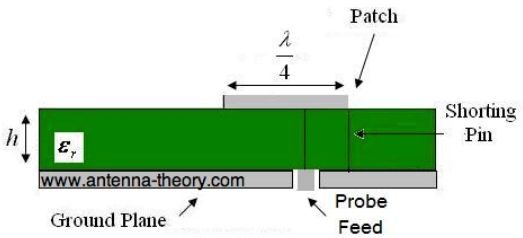

Figure 2.3: The Planar Inverted-F Antenna (PIFA) [28].

The PIFA is resonant at a quarter-wavelength because of the shorting pin at the end. We will

see how the resonant length is defined exactly in a minute. The input is placed between the open and short end, and the position controls the input impedance. In PIFAs, the shortening pin can be a plate, as shown in Figure 2.6:

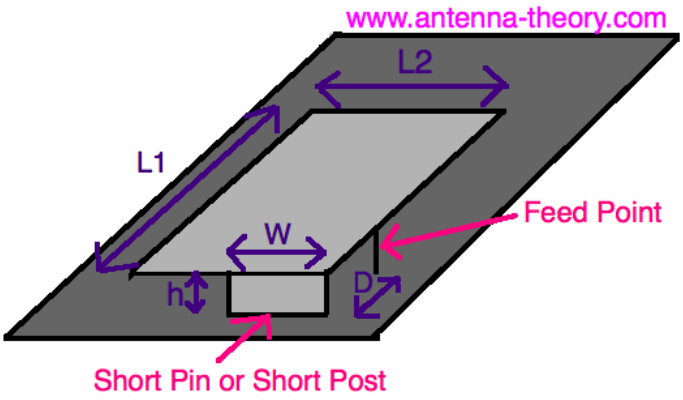

Figure 2.4: The Planar Inverted-F Antenna (PIFA), with a shorting Plane [28].

In Figure 2.4, we have a PIFA of length L1, of width L2. The shortening pin (or shortening post) is width W and begins at one edge of the PIFA as shown in Figure. The input point is along the same edge as shown. The feed is a distance D from the shorting pin. The PIFA is at a height h from the ground plane. The PIFA sits on top of a dielectric with permittivity ε_r as with the patch antenna. The impedance of the PIFA can be controlled via the distance of the feed to the short pin (D). The closer the feed is to the shorting pin, the impedance will decrease; the impedance can be increased by moving it farther from the short edge. The PIFA can have it's impedance tuned with this parameter. The resonant frequency of the PIFA depends on W. If W=L2, then the shortening pin runs the entire width of the patch. In this case, the PIFA is resonant (has maximum radiation efficiency) when:

$$\text{if } W = L2 \implies L1 = \frac{\lambda}{4} \tag{2.12}$$

Suppose that $W = 0$, so that the short is just a pin (or assume $W << L2$). Then the PIFA is resonant at:

$$\text{if } W = 0 \implies L1 + L2 = \frac{\lambda}{4} \tag{2.13}$$

The resonant length of the PIFA depends on the shortning pin length W Intuitively, think

about how a quarter-wavelength patch antenna radiates. It needs a quarter-wavelength of space between the edge and the shorting area. If W=L2, then the distance from one edge to the short is simply L1, which gives us Equation 2.12. when W=0. Since the fringing fields along the edge give rise to radiation in microstrip antennas, we see that the length from the open-circuited radiating edge (the far edge in Figure 2.3) to the shorting pin is on average equal to $L1 + L2$. You can convince yourself of this by measuring the distance from any point on the far edge of the PIFA to the shorting pin. The clockwise and counter-clockwise paths always add up to $2(L1 + L2)$, so on average resonance will occur when the path length $(L1 + L2)$ for a single path is a quarter-wavelength. In general, we can approximate the resonant length of a PIFA as a function of it's parameters as:

$$L1 + L2 - W = \frac{\lambda}{4} \tag{2.14}$$

In Equation 2.14, note that we used one of the fundamental antenna equations, which relates wavelength, speed of light, and permittivity.

$$C = \lambda f \tag{2.15}$$

$$f = \frac{C_0}{\lambda\sqrt{\varepsilon_r}} = \frac{3.10^8}{\lambda\sqrt{\varepsilon_r}} \tag{2.16}$$

2.4 Microstrip Feed Types

The four most commonly used feeding techniques are the microstrip line, the coaxial probe (both contact schemes), the aperture coupling, and the proximity coupling (both non-contact schemes).

2.4.1 Microstrip Line Feed

In this type of feeding technique, a conductive strip is directly connected to the edge of the patch as shown in the figure below. This type of Feed arrangement has the advantage that the feed can be etched onto the same substrate to produce a planar structure. An internal cutout can be integrated into the patch to achieve good impedance matching without requiring an additional matching element. However, as the thickness of the dielectric substrate increases,

the surface waves and scattered radiation also increase, hindering the bandwidth of the antenna. This type of feeding leads to unwanted cross-polarization effects.

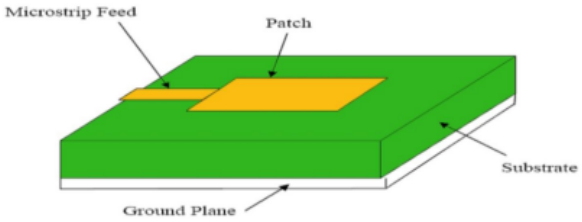

Figure 2.5: microstrip line feed [29]

2.4.2 Coaxial Feeding

The internal conductor of the coaxial connector extends through the dielectric and is soldered to the radiation patch, while the outer conductor is connected to the ground plane. The main advantage of this type of feeding scheme is that the feed can be placed at any desired location in the patch to achieve impedance matching. This feed method is easy to fabricate and has low stray radiation effects.

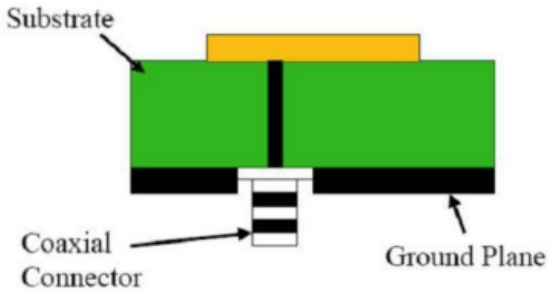

Figure 2.6: coaxial feed [29]

2.4.3 Aperture-Coupling

The radiating patch element is etched on the top of the antenna substrate and the microstrip feed line is etched on the bottom of the feed substrate to obtain the aperture coupling. Therefore, the thickness and dielectric constant of these two substrates can be chosen independently to optimize the separate electrical functions of radiation and circuitry. The coupling aperture is typically centered below the patch, resulting in lower cross-polarization due to the symmetry of the configuration.

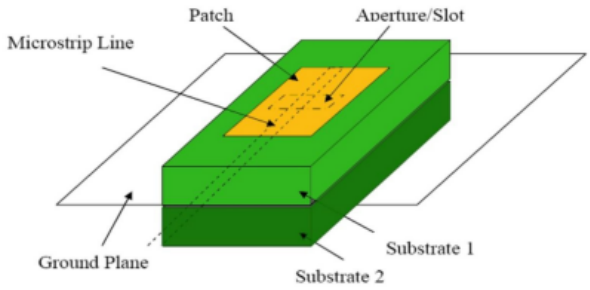

Figure 2.7: aperutre couple feeding [29]

2.4.4 Proximity Coupling

Is an electromagnetic coupling.The two dielectric substrates are used so that the power line is between the two substrates and the radiation region is on the other side on the substrate above. The main advantage of this feeding technique is that it eliminates scattered radiation and provides a very high bandwidth as a result of the increased electrical thickness of the patch antenna.

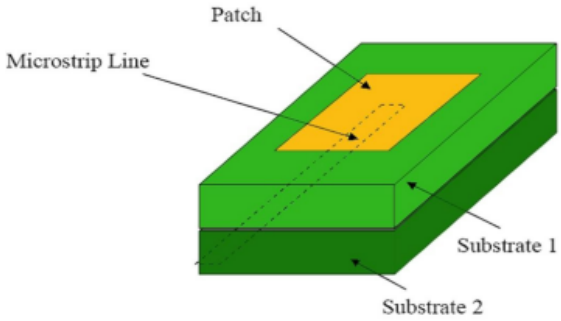

Figure 2.8: aperutre couple feeding [29]

2.5 Bandwidth Enhancement Techniques

2.5.1 Slot Loading

The integration of slots into the patch of a millimeter-wave PIFA antenna is a widely adopted technique to improve its bandwidth. Slots or slits introduce additional resonances by altering the current distribution, which effectively expands the operating bandwidth without significantly increasing the size of the antenna. This method exploits the concept of multi-resonance coupling, where additional structures such as cavities or resonant paths complement the primary resonance of the PIFA. As a result, the antenna achieves better

impedance in a wider frequency range. In addition, the position, size, and shape of the slots are critical parameters that are meticulously optimized to ensure minimal loss of radiation efficiency while maintaining compactness[30]. In other words, the bandwidth of a microstrip or PIFA antenna is governed by the quality factor (Q) and impedance matching.

$$\text{BW} \approx \frac{f_0}{Q} \tag{2.17}$$

Where:

- BW = Bandwidth
- f_0 = Resonant frequency
- Q = Quality factor

The lower the Q, the wider the bandwidth. For a basic PIFA, the Q is relatively high because of limited radiation and narrow impedance matching. Slot loading introduces additional resonances and alters the current distribution, effectively Lowering the Q, Creating multiple nearby resonances, and improving impedance matching across a wider range. Mathematically, adding a slot modifies the effective electrical length of the patch.

2.5.1.1 Without Slot

The fundamental resonant frequency of a rectangular PIFA is approximately:

$$f_0 = \frac{c}{2L_{\text{eff}}\sqrt{\varepsilon_r}} \tag{2.18}$$

Where:

- c = speed of light
- L_{eff} = Effective length of patch
- ε_r = Relative permittivity of substrate

2.5.1.2 With Slot

When a slot of length ΔL_s is added:

$$L_{\text{eff,new}} = L + \Delta L_s \tag{2.19}$$

$$f_s = \frac{c}{2\,(L + \Delta L_s)\,\sqrt{\varepsilon_r}} < f_0 \tag{2.20}$$

This leads to a new resonance at a lower frequency.

If the slot is carefully designed, it can support its own resonance, and the impedance bandwidth becomes the range that includes both frequencies.

$$f_s \approx f_0 \tag{2.21}$$

- f_0: Main patch mode
- f_s: Slot-induced mode

These two resonances overlap and create Superposition of Resonances to broadening the overall bandwidth.

The input impedance of a slot-loaded patch is altered With slot loading, the imaginary part $X(f)$ is adjusted near multiple frequencies, leading to better matching across a larger band. A lower $|\Gamma(f)|$ across more frequencies implies a wider bandwidth.

$$Z_{\text{in}}(f) = R(f) + jX(f) \tag{2.22}$$

$$\Gamma(f) = \frac{Z_{\text{in}}(f) - Z_0}{Z_{\text{in}}(f) + Z_0} \tag{2.23}$$

2.5.2 Using a parasitic element

Improve the bandwidth of a millimeter-wave PIFA by changing its radiation characteristics. These elements, usually located near the radiation patch, interact with electromagnetic fields to create additional resonances. By carefully designing the size, position, and coupling of the parasitic elements, the antenna can achieve a wider impedance bandwidth, effectively adapting to a wider frequency range. Parasitic elements improve impedance matching and broaden the frequency spectrum without increasing the overall footprint of the antenna. In [31] The enhancement occurs due to the mutual coupling between the main part and the parasitic elements, which shifts and broadens the resonance modes.

The length of the parasitic element is generally related to the wavelength at the operating frequency. It is often chosen to be slightly less than or equal to a quarter of the guided wavelength ($\lambda_g/4$) to create a resonant condition:

$$L_p = \frac{\lambda_g}{4} \tag{2.24}$$

$$\lambda_g = \frac{\lambda_0}{\sqrt{\varepsilon_r}} \tag{2.25}$$

- $\lambda_0 = \frac{c}{f}$: Free-space wavelength
- c: Speed of light ($3 \times 10^8\,\mathrm{m/s}$)
- f: Operating frequency;
- ϵ_r: Relative permittivity of the substrate

The width of the parasitic element affects the impedance matching and is generally chosen to be smaller than the width of the main radiating element Fine-tuning is required for improved bandwidth and coupling to the main patch

$$W_p \approx 0.1\lambda_g\text{–}0.2\lambda_g \tag{2.26}$$

The height of the parasitic element above the ground plane influences the coupling and

impedance. It is generally chosen as a fraction of the substrate height

$$h_p = h_s + \Delta h \tag{2.27}$$

where:

- h_s: Substrate height
- Δh: Additional height (typically a small fraction, approximatly, 0.05λ) to optimize coupling and bandwidth.

Spacing Between PIFA and Parasitic (d) and thickness of the parasite

$$d = \frac{\lambda}{10} \text{ to } \frac{\lambda}{20} \tag{2.28}$$

$$(h + t) - d = 0.105\lambda \tag{2.29}$$

Where:

- h = thickness of the substrate,
- d = distance between the patch and the element,
- t = thickness of the parasite.

2.5.3 Deffective Ground Structure (DGS)

A Defected Ground Structure (DGS) enhances the bandwidth (BW) of a mmWave PIFA antenna by introducing slots or patterns in the ground plane, which disrupt the current distribution and increase the effective inductance and capacitance. This alteration modifies the antenna's input impedance, suppresses surface waves, and reduces mutual coupling, leading to improved impedance matching over a wider frequency range.

2.5.3.1 Without DGS

with out DGS the input impedance of a basic PIFA can be approximated using transmission line theory.

$$Z_{in} = R + jX = Z_0 \frac{Z_L + jZ_0 \tan(\beta l)}{Z_0 + jZ_L \tan(\beta l)} \tag{2.30}$$

where:

- Z_0: characteristic impedance
- Z_L: Load impedance at the shorted pin
- $\beta = \frac{2\pi}{\lambda}$: Phase constant;
- l: Effective electrical length

2.5.3.2 With DGS

The introduction of a DGS modifies the path of the ground current, introducing additional inductance (L) and capacitance (C). This can be modeled as an LC resonator in the ground plane:

$$Z_{\text{DGS}}(f) = j\omega L - \frac{j}{\omega C} \tag{2.31}$$

The effective input impedance becomes:

$$Z_{\text{in}}^{\text{DGS}} = Z_{\text{in}} + Z_{\text{DGS}}(f) \tag{2.32}$$

This changes the resonance condition and adds multiple resonant modes. The matching condition is improved over a broader frequency range, increasing the bandwidth.

2.5.4 Improving The Parameters

The dimensions of the shortening plate and the thickness of the substrate material serve as two essential physical factors that can directly impact the impedance bandwidth of a millimeter wave PIFA. Enlarging the width of the shorting plate decreases the inductive

reactance and minimizes the overall Q-factor of the resonant cavity established between the radiating patch and the ground. This adjustment results in reducing the narrow-band characteristics of the antenna and enhances wideband matching around 28 GHz. A broader shortening plate also improves the uniformity of current distribution, thus diminishing the pronounced resonance peaks that typically restrict usable bandwidth. By optimizing the thickness of the substrate and ensuring that it is not excessively large to prevent surface-wave losses, the antenna can achieve a more consistent input impedance over an extended frequency range. Consequently, the concerent adjustment of the width of the shorted plate and the thickness of the substrate significantly enhances the bandwidth.The fractional bandwidth (FBW) of a resonant antenna is inversely proportional to its quality factor [32].

$$\text{FBW} \approx \frac{1}{Q}, \qquad Q = \omega_0 \frac{W_{\text{stored}}}{P_{\text{rad}}} \tag{2.33}$$

2.5.4.1 Effect of Shortening Plate Width

In a PIFA, the shorting plate introduces inductive loading between the radiating patch and the ground plane. The inductance of the shorting plate can be approximated by [33]:

$$L_s \approx \mu_0 h \left(\ln \frac{2h}{w_s} + 0.5 \right) \tag{2.34}$$

where h is the thickness of the substrate and w_s is the width of the shortening plate. Increasing the width of the shorting plate reduces the inductance:

$$w_s \uparrow \Rightarrow \; L_s \downarrow \tag{2.35}$$

The input reactance near resonance is given by:

$$X(\omega) = \omega L_s - \frac{1}{\omega C} \tag{2.36}$$

A reduction in L_s decreases the slope $\mathrm{d}X/\mathrm{d}\omega$, resulting in a lower inductive quality factor:

$$Q_L = \frac{\omega_0 L_s}{R_{\text{rad}}} \downarrow \tag{2.37}$$

which leads to an enhanced impedance bandwidth.

2.5.4.2 Effect of Substrate Thickness

The stored electric energy in the substrate is expressed as [32]:

$$W_e = \frac{1}{2} \int \epsilon |E|^2 \, dV \tag{2.38}$$

Reducing the substrate thickness lowers the stored energy:

$$h \downarrow \Rightarrow \; W_{\text{stored}} \downarrow \tag{2.39}$$

Additionally, surface-wave power supported by a dielectric substrate scales approximately as [34]:

$$P_{\text{sw}} \propto h^3 \tag{2.40}$$

Thus, a thinner substrate suppresses surface waves and increases the radiated power, reducing the overall quality factor:

$$Q = \omega_0 \frac{W_{\text{stored}}}{P_{\text{rad}}} \downarrow \tag{2.41}$$

Thus,

$$\boxed{w_s \uparrow \text{ and } h \downarrow \Rightarrow \; L_s \downarrow, \; W_{\text{stored}} \downarrow, \; Q \downarrow \Rightarrow \text{ Bandwidth increases}} \tag{2.42}$$

Chapter 3

3.1 Design of PIFA Antenna

To design a planar inverted F antenna, the necessary parameters are the operating frequency of the antenna (f_r), the relative dielectric constant of the substrate (ε_r), and the thickness of the electrical substrate (h). The selection of these parameter design parameters is very important because the size of the PIFA antenna and the performance of the antenna depend on these parameters. To obtain a high data rate for mobile 5G communication, the selected resonant frequency for the design is 28 GHz. The dielectric material selected for the design is RT5880, which has a dielectric constant of 2.2. [35] To use the PIFA antenna in the mobile phone, the antenna must not be large. The performance of a PIFA antenna depends on its size. Radiation efficiency, reflection attenuation, gain, directivity, and other related parameters are affected depending on the patch size. For effective radiation, the actual width of the patch can be calculated as [36].

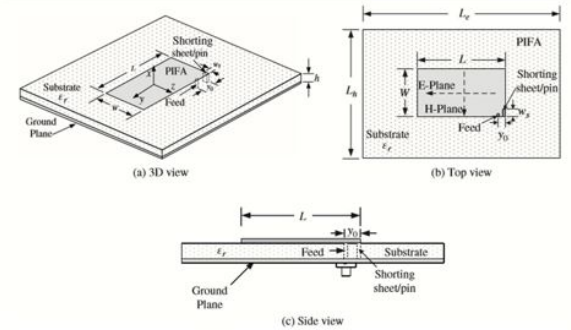

Figure 3.1: Basic PIFA Geometry [37].

3.1.1 Antenna Design Specification

Specifications for the normal design of single element PIFA is:

- Type of antenna: inverted planar F antenna
- Resonance frequency: 28 GHz.
- Input impedance: 50-ohm.
- Feeding method: coaxial prob Feed
- Material for the radiating element: copper
- The dimension of the radiating patch is L_p and W_p
- The dimension of the ground plane is L_g and W_g
- Substrate Dielectric constant: $\varepsilon_r = 2.2$ (FR-4)

3.1.2 Parameters of the PIFA antenna

Patch Width (W)

The practical width of the patch used is calculated using the equation

$$W = \frac{c}{2f\sqrt{\frac{\varepsilon_r+1}{2}}} \tag{3.1}$$

The Effective Dielectric Constant(ε_{eff})

The effective dielectric constant of the PIFA antenna is given by:

$$\varepsilon_{\text{eff}} = \frac{\varepsilon_r + 1}{2} + \frac{\varepsilon_r - 1}{2}\left[1 + \frac{12h}{W}\right]^{-1/2} \tag{3.2}$$

The Effective Length (L_{eff}): The length of the patch looks electrically slightly larger than the usual length of the design due to the fringing field along the patch width:

$$L_{\text{eff}} = \frac{c}{2f_0\sqrt{\varepsilon_{\text{eff}}}} \tag{3.3}$$

The extension of the length (ΔL): Due to the fringing fields along the antenna, it is appropriate to use an extended length for better performance. The length is extended by ΔL as given below:

$$\Delta L = 0.412h \cdot \frac{\varepsilon_{\text{eff}} + 0.3\left(\frac{w}{h} + 0.264\right)}{\varepsilon_{\text{eff}} - 0.258\left(\frac{w}{h} + 0.8\right)} \tag{3.4}$$

Actual length of the patch (L): After the calculation of each of the effective and extended lengths of the patch, the actual value of the radiating patch length (L) is given by:

$$L = L_{\text{eff}} - 2\Delta L \tag{3.5}$$

Dimensions of the ground plane (L_g and W_g): The transmission line model is applicable only to infinite ground planes. However, for practical considerations, it is basic to have a finite ground plane. It is shown by [38] that comparable results can be obtained for finite and infinite ground planes if the size of the ground plane is greater than the patch dimensions by approximately six times the thickness of all whole substrate around the periphery. Hence, for this structure, the ground plane measurements would be given as:

$$L_g = 6h + L, \quad w_g = 6h + w \tag{3.6}$$

The location of the feeding probe point can be located at the point (X_f, Y_f) in the coordinates x-y. The location points are given by the equations below. They achieved low input impedance or good line and port synchronization [38].

$$X_f = \frac{L}{\sqrt{2 \cdot \varepsilon_{\text{reff}}}} \tag{3.7}$$

$$Y_f = \frac{w}{2} \tag{3.8}$$

Where X_f and Y_f are the desired input feed points on the x-axis and the y-axis, respectively. They were neglected because they represent the position on the edge of the patch antenna and were more suitable for feeding through a microstrip feed line [36].

w = width of the patch antenna

L = length of the patch antenna

f_0 = resonance frequency

c = speed of light

ε_r = dielectric constant of the substrate

L_{eff} = effective length

ΔL = length extension

h = thickness of the substrate

ε_{eff} = effective dielectric constant of the substrate

The input point must be located at a point in the patch with an input impedance of 50 ohms with respect to the resonant frequency. 50 ohms is an excellent compromise between power handling and low loss, for the air dielectric coax. For different feed point locations, the return loss (RL) is compared and this point, and the power source is chosen where RL is the most negative. Often a match between the feedline and the antenna is required. This is because the antenna input impedance differs from the typical line impedance of 50Ω. Matching can be achieved by choosing the correct location of the feed line. Because probe feeding is used, several parameters must be calculated. The matching impedance used is 50Ω. To match this impedance, the connector must be placed a distance from the edge corresponding to 50Ω. The following equations were used to calculate the exact position of the port. The free-space wavelength is given by

$$\lambda_0 \approx \frac{c}{f_r} \tag{3.9}$$

where c is the speed of light and f_r is the resonant frequency.

The wave number and related input impedance parameters can be expressed as

$$G_1 = \frac{w}{120\,\lambda_0}\left[1 - 2\left(\frac{1}{24}\right)k^2\right] \tag{3.10}$$

$$Z_{\text{in}} = \frac{1}{G_1} \tag{3.11}$$

$$R_{\text{in}} = \cos^{-1}\left(\sqrt{\frac{Z_0}{Z_{\text{in}}}}\right)\frac{l}{\pi} \tag{3.12}$$

Where w and l = width and length of the patch $k = 1.380658^{-}23$ The feed point must be located at a point in the patch with an input impedance of 50 ohms with respect to the resonant frequency. 50 ohm is an excellent compromise between power handling and low loss, for air dielectric coax.

PIFA Design Calculation

The three essential parameters for the design of a PIFA antenna are:

- Frequency of Operation (f_r): the resonant frequency of the antenna must be selected appropriately. 28 GHz
- Dielectric Constant of the Substrate (ε_r): the dielectric material applied for this design has a dielectric constant of 2.2
- Height of the dielectric substrate (h): for the antenna to be used in cellular phones, it is essential that the antenna is not bulky. Hence, the height of the dielectric substrate selected here is 0.6 mm.

Hence, the essential parameters for the design are:

$$f_r = 28 \text{ GHz}$$
$$\varepsilon_r = 2.2$$
$$h = 0.45 \text{ mm}$$

Step 1: Calculation of the Width (W):

$$W = \frac{c}{2f_r\sqrt{\frac{\varepsilon_r+1}{2}}} \tag{3.13}$$

The width of the PIFA antenna is given as: Substituting $c = 3.00 \times 10^8$ m/s, $\varepsilon_r = 2.2$, and $f_o = 28$ GHz, we get:

$$W = 4.235 \text{ mm}$$

Step 2: Calculation of the effective dielectric constant (ε_{eff}):

$$\varepsilon_{\text{eff}} = \frac{\varepsilon_r + 1}{2} + \frac{\varepsilon_r - 1}{2}\left[1 + 12\frac{h}{W}\right]^{-1/2} \tag{3.14}$$

Substituting $\varepsilon_r = 2.2$, $W = 4.235$ mm, and $h = 0.6$ mm, we get:

$$\varepsilon_{\text{eff}} = 2.3156$$

Step 3: Calculation of the Effective length

$$L_{\text{eff}} = \frac{c}{2f_0\sqrt{\varepsilon_{\text{eff}}}} \tag{3.15}$$

Substituting $\varepsilon_{\text{eff}} = 2.3156$, $c = 3.00 \times 10^8$ m/s and $f_o = 28$ GHz, we get:

$$L_{\text{eff}} = 2.4172 \text{ mm}$$

Step 4: Calculation of the length extension (ΔL):

$$\Delta L = 0.412h\left(\frac{\varepsilon_{\text{eff}} + 0.3}{\varepsilon_{\text{eff}} - 0.258}\right)\left(\frac{W/h + 0.264}{W/h + 0.8}\right) \tag{3.16}$$

Substituting $\varepsilon_{\text{eff}} = 2.3156$, $W = 4.235$ mm, and $h = 0.6$ mm, we get:

$$\Delta L = 0.32 \text{ mm}$$

Step 5: Calculation of the actual length of the patch (L):

$$L = L_{\text{eff}} - 2\Delta L \tag{3.17}$$

Substituting $L_{\text{eff}} = 2.4172$ mm and $\Delta L = 0.32$ mm, we get:

$$L = 1.7772 \text{ mm}$$

Step 6: Calculation of the dimensions of the ground plane (L_g and W_g):

$$L_g = 6h + L = 3.606 \text{ mm} \tag{3.18}$$

$$W_g = 6h + W = 4.829 \text{ mm} \tag{3.19}$$

Where L_g and W_g are the length and width of the substrate and h is given by the equation

$$h = \frac{0.0606\lambda}{\sqrt{\varepsilon_r}} = 0.437 \text{ mm}$$

Step 7: Calculation for radiating Patch dimension from equation

$$W_p = \frac{c}{4f\sqrt{\varepsilon_r}} = 1.81 \text{ mm} \tag{3.20}$$

$$L_p = \frac{c}{4f} = 2.679 \text{ mm} \tag{3.21}$$

Step 8: Calculation of the distance between the shortening plate and a parasite

$$d = \frac{\lambda}{10} \text{ to } \frac{\lambda}{20} \approx 1.07 \text{ mm to } 0.54 \text{ mm} \tag{3.22}$$

Step 9: Calculation for the dimention of a parasite element

$$\lambda_g = \frac{\lambda_0}{\sqrt{\varepsilon_r}} = 7.22 \text{ mm} \tag{3.23}$$

$$W_p \approx 0.1\lambda_g - 0.2\lambda_g \approx 0.72 \text{ mm} - 1.44 \text{ mm} \tag{3.24}$$

$$h_p = h_s + \Delta h = 0.45 \text{ mm} + 0.54 \text{ mm} = 0.99 \text{ mm} \tag{3.25}$$

Table 3.1: The calculated physical dimensions of a mm wave PIFA antenna

No	Parameters	Symbols	Calculated Value (mm)
1	Width of the Ground Plane	W_g	4.829
2	Length of the Ground Plane	L_g	3.606
3	Width of the Patch	W_p	4.23
4	Length of the Patch	L_p	1.7772
5	Shortening Plate Width	W_{sp}	0.450
6	Thickness of Substrate	h	0.45
7	Feed Position	(x_0, y_0)	1.0475, 1.25
8	Air Gap	h_g	0.6
9	Inner & Outer Radius	R_i, R_o	0.118, 0.254
10	width of parasite	W_p	0.72-1.44
11	Height of parasite	h_p	0.99
12	slot thickness	S_t	0.1

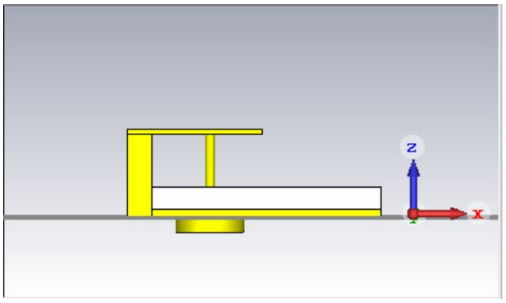

a Initial conventional single-element mmWave PIFA antenna.

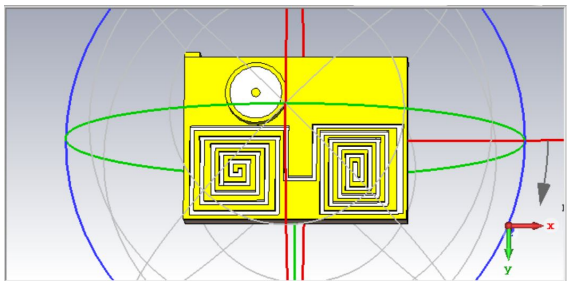

b DGS single-element mmWave PIFA antenna.

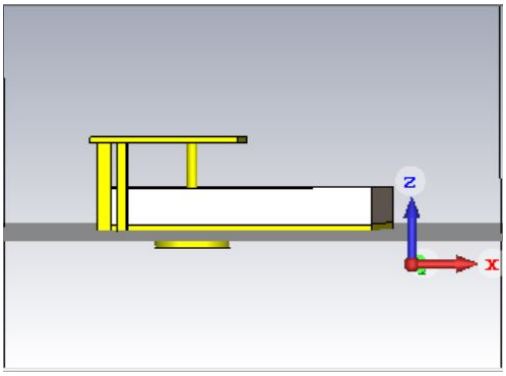

c Parasitic single-element mmWave PIFA antenna.

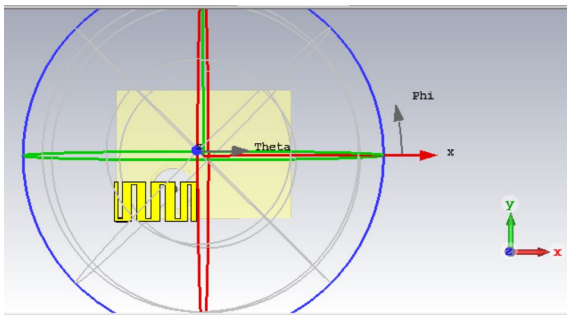

d Slotted single-element mmWave PIFA antenna.

Figure 3.2: Models of different single-element mmWave PIFA antenna designs.

Chapter 4

Results And Discussions

After appropriately selecting substrate materials, representing the design parameters and creating the PIFA antenna, all of the configurations established in the preceding chapter are computer simulated using CST simulation software. By varying different parameters at the same operating frequency of the substrate material, the corresponding gain, directivity, return loss, beam width, bandwidth, and radiation pattern of polarized PIFA antennas for single-element, parasitical,DGS,Sloted, improved the width of shorthning plate and the thickness of the substrate of a mm wave PIFA antennas are computed by performing relevant computer simulations for each of these situations separately.

In this research, it was required to analyze one of the basic parameters that should be recommended with appropriate dimensions with the desired band frequency for mobile communication systems. Based on the mathematical models, the important parameters are analyzed using the CST software.

4.1 Study Effects of the BW Enhancement Techniques

4.1.1 Effects of Improved Ws and h

The influence of the physical dimensions of the antenna on the achievable bandwidth was investigated. When the antenna substrate height increased from $h = 0.40$ mm to $h = 0.425$ mm and $h = 0.45$ mm, the impedance bandwidth improved by approximately 423.3 MHz and 569 MHz, respectively. Similarly, modifying the width of the plate from $w_s = 0.40$ mm

to $w_s = 0.475$ mm and $w_s = 0.50$ mm resulted in an additional bandwidth enhancement of around 265 MHz and 389 MHz. These results confirm that increasing both height and width strongly contributes to a broader operational bandwidth in the proposed antenna design. and all other design parameters should be varied depending on the dimensions of W_s as well as h.

4.1.2 Effect of Parasitic Element

An ”l”-shaped parasitic elements are strategically placed to improve key performance metrics such as minimizing return loss S11 to -25.5dB, increasing the bandwidth to 841MHz and the efficiency to 61.5% with a gain of 2.693dB.The impact of parasitic on the parameters of the PIFA antenna, particularly at high frequencies, is shown in the figure below. By optimizing the placement and dimensions of parasitic elements, the overall efficiency and radiation characteristics of the antenna can be enhanced.

4.1.3 Effect of Slot Loading

The zigzag geometry slot increases the effective current path without enlarging the antenna size, introducing multiple nearby resonances. These additional resonant modes overlap with the fundamental frequency, resulting in improved impedance matching and widening of a bandwidth of 751MHz, a gain of 2.823dB and an efficiency of 67%. The slot's meandering structure also promotes better surface current distribution, reducing the Q quality factor and allowing broader operation.

4.1.4 Effect of DGS

Incorporate intentional spaces or patterns into the ground plane, affecting the distribution of the surface current. This alters the effective inductance and capacitance of the antenna, lowering the Q factor and enabling multiple or wider resonances. At millimeter Wave frequencies. It improves impedance matching and reduces mutual coupling, which broadens the bandwidth of 841MHz with a gain of 2.916dB. The modified ground also increases the current path, effectively increasing the total efficiency of 62%. As a result, DGS is a compact and efficient method to meet the wideband requirements of 5G mobile communication systems.

4.2 Antenna Parameters

4.2.1 Return Loss (S11)

Among the bandwidth enhancement techniques, the DGS method shows the best return loss with S11 = -29.75dB, indicating better impedance matching. The slotted and parasaitic methods follow with -27dB and -25.5dB respectively. while the improved parameters of ws and h were enhanced the return loss to -15.437dB and -14.6dB while the conventional PIFA has a return loss of -14dB.The simulation results were shown in the fig below.

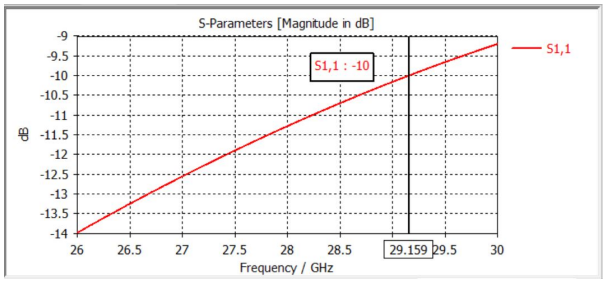

Figure 4.1: Return loss (S11) of conventional mm-wave single-element PIFA antenna

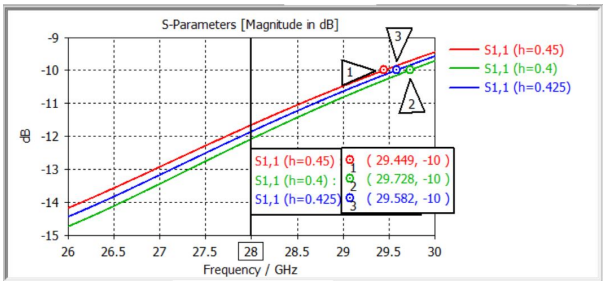

Figure 4.2: Return loss (S11) of height-improved mm-wave single-element PIFA antenna

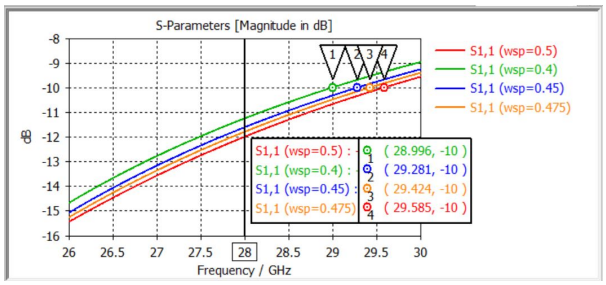

Figure 4.3: Return loss (S11) of width-slot improved mm-wave single-element PIFA antenna

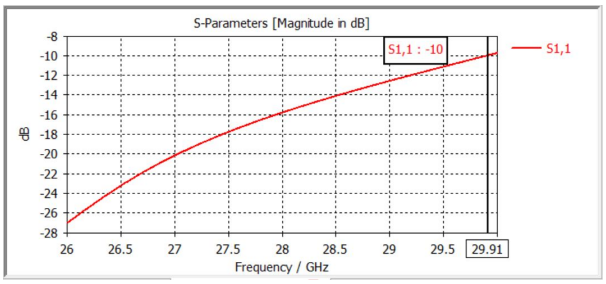

Figure 4.4: Return loss (S11) of slot-loaded mm-wave single-element PIFA antenna

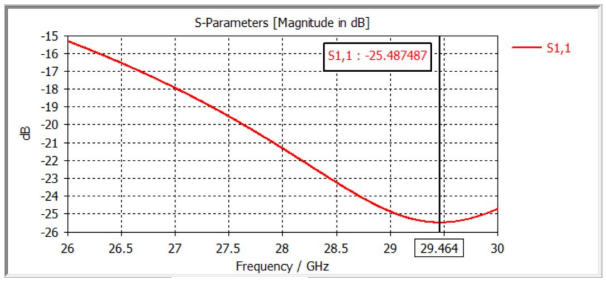

Figure 4.5: Return loss (S11) of DGS-based mm-wave single-element PIFA antenna

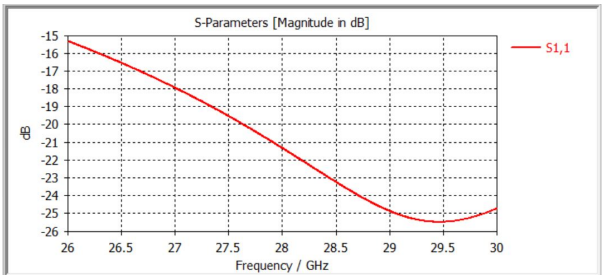

Figure 4.6: Return loss (S11) of parasitic-loaded mm-wave single-element PIFA antenna

4.2.2 Gain

The Defected Ground Structure (DGS) technique yields the highest gain at 2.916dB, indicating improved radiation efficiency and bandwidth.The conventional design has a gain of 3.371dB serving as a baseline. The slot loading technique achieves a slightly lower gain of 2.823dB, suggesting moderate enhancement. Meanwhile, the design of parasitic elements shows the lowest gain at 2.693dB, potentially due to increased surface currents and losses . Overall, improving Ws methods provides a good gain of 3.198dB and is the most effective among the listed methods in enhancing gain and potentially bandwidth performance.

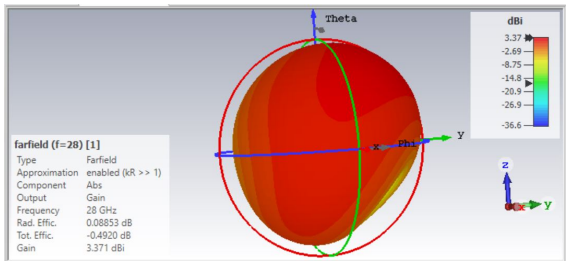

Figure 4.7: Gain of a mm-wave single element PIFA antenna

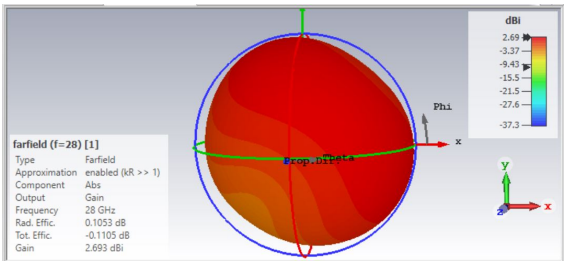

Figure 4.8: Gain of a parasitic-loaded mm-wave PIFA antenna

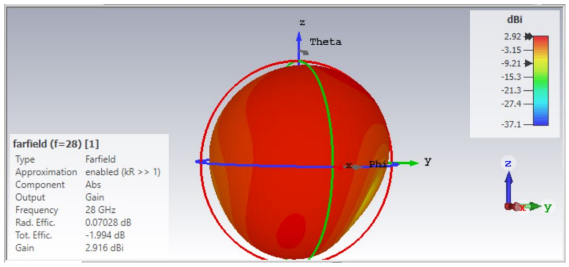

Figure 4.9: Gain of a DGS mm-wave single element PIFA antenna

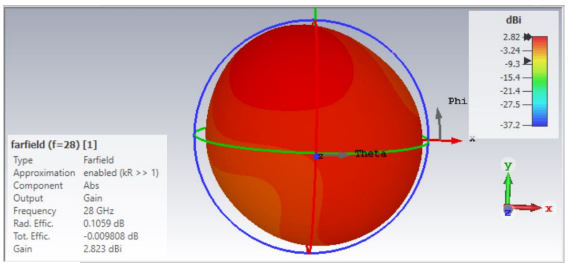

Figure 4.10: Gain of a slotted mm-wave single element PIFA antenna

4.2.3 Radiation Pattern

The radiation pattern of a millimeter-wave Planar Inverted-F Antenna PIFA is critical to understanding its performance. The angle beam width at 3dB reflects the radiation spread. The DGS, the slotted and the parasited antenna show the widest beam width of 141.4°, 191.1°and 141.7° the improved h and ws antennas covered 119.1° and 124.3° are beneficial for broad coverage. slot loading provides a balanced trade-off between coverage and directionality. The magnitude of the main lobe indicates the maximum radiation strength. The slotted antenna has the lowest magnitude of the main lobe of 2.41dB, suggesting the trade off between bandwidth enhancement and gain. In contrast, the DGS design achieves the highest 3.54dB,

and the parasited antenna has 3.24dB, which is ideal for focused transmission. Thus,both designs better support 5G applications where both bandwidth and directional gain are crucial.

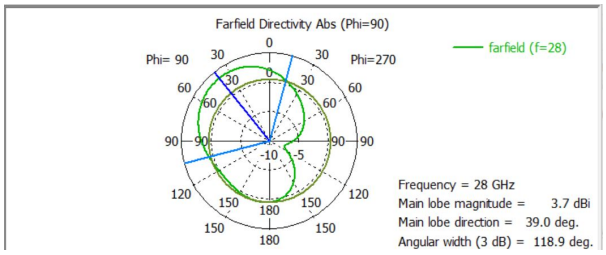

Figure 4.11: Far field ($\phi = 90°$) of conventional mm-wave PIFA

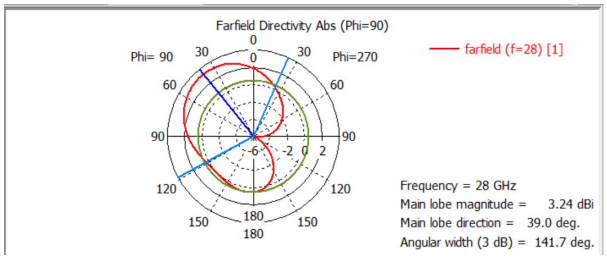

Figure 4.12: Far field ($\phi = 90°$) of parasitic-loaded mm-wave PIFA

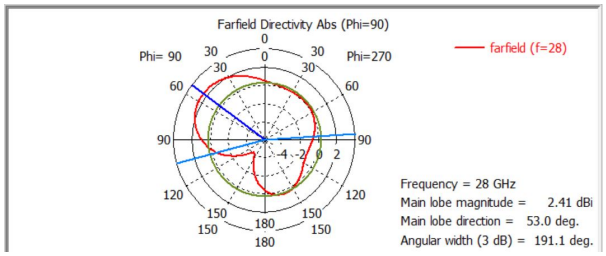

Figure 4.13: Far field ($\phi = 90°$) of slotted mm-wave PIFA

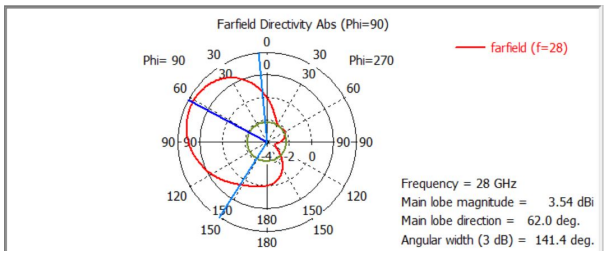

Figure 4.14: Far field ($\phi = 90°$) of DGS mm-wave PIFA

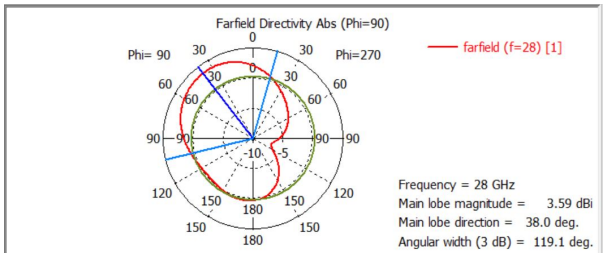

Figure 4.15: Far field ($\phi = 90°$) of height-improved mm-wave PIFA

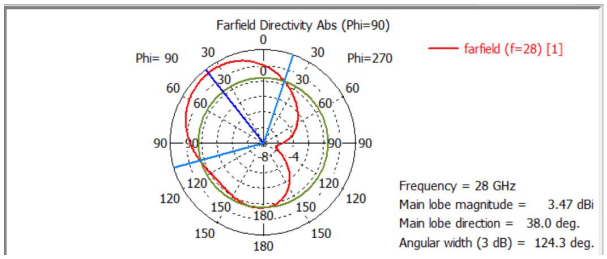

Figure 4.16: Far field ($\phi = 90°$) of width-improved mm-wave PIFA

4.2.4 Efficiency

The efficiency comparison of bandwidth-enhancement techniques for the mmWave PIFA antenna highlights clear trade-offs between bandwidth improvement and radiation performance for 5G mobile applications. The conventional PIFA shows a relatively high efficiency of 74.7% but lacks bandwidth enhancement, making it unsuitable for wideband 5G requirements. The improvement in height h provides dual-band enhancement, but reduces efficiency to 68.5%, indicating increased losses. The width W_s improvement achieves one of the highest efficiencies 76%, showing that moderate geometric tuning can enhance the bandwidth while preserving radiation efficiency. Slot loading significantly increases bandwidth; however, efficiency drops

to 64.5% due to higher surface current disruption. Defected Ground Structure (DGS) and parasitic methods offer the largest bandwidth enhancement 841 MHz, but suffer the lowest efficiencies 61%, as ground perturbations and mutual coupling introduce additional losses. In general, W_s offers the best balance of bandwidth efficiency, while DGS and parasitic techniques prioritize bandwidth enhancement at the expense of radiation efficiency.

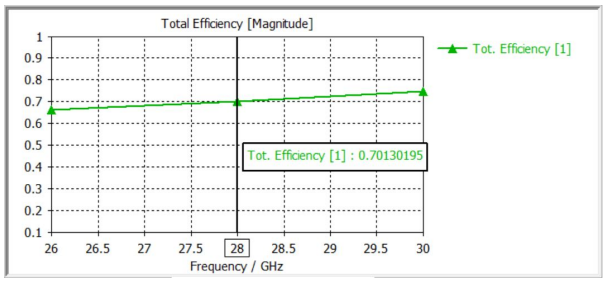

a Conventional PIFA

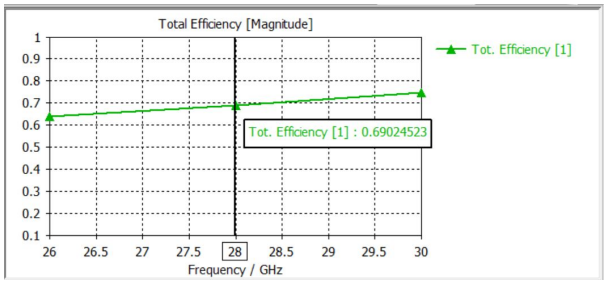

b Improved h PIFA

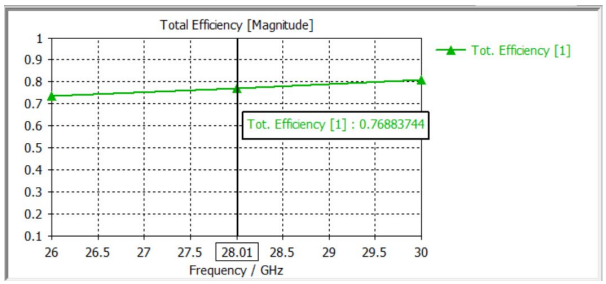

c Improved w_s PIFA

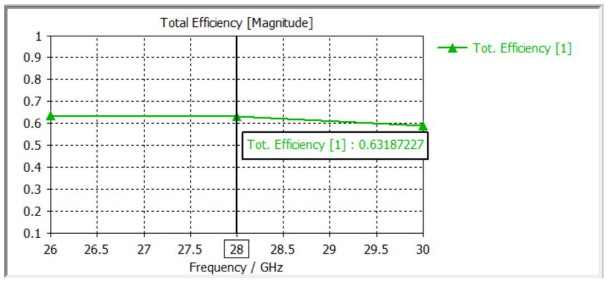

d DGS PIFA

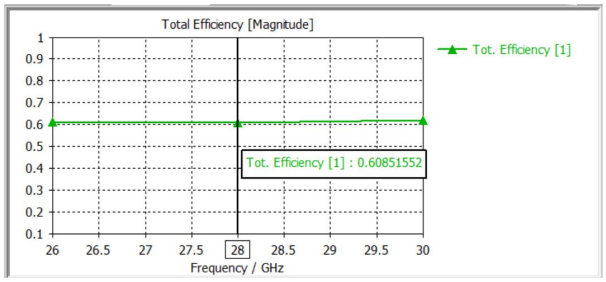

e Parasitic-loaded PIFA

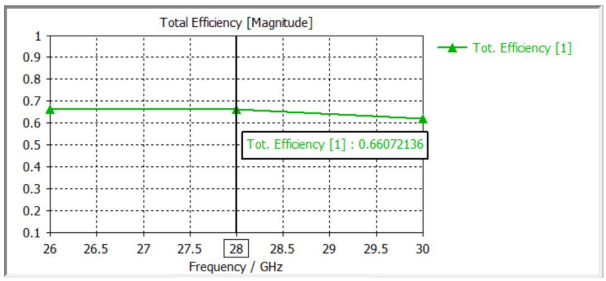

f Slotted PIFA

Figure 4.17: Total efficiency comparison of different mm-wave single-element PIFA antenna configurations

4.2.5 VSWR

VSWR values indicate their effectiveness in impedance matching. The data shows that conventional PIFA has a VSWR of 1.8, which is moderate, while the H-improved and Ws-improved designs reduce it to 1.73 and 1.44, respectively, indicating better impedance matching. Slot loading and DGS techniques further lower VSWR to 1.42 and 1.07, showing

significantly improved matching and bandwidth. The parasitic method also achieves low VSWR (1.112). Overall, advanced techniques like DGS and slot loading provide the best VSWR performance for mmWave 5G PIFA antennas.

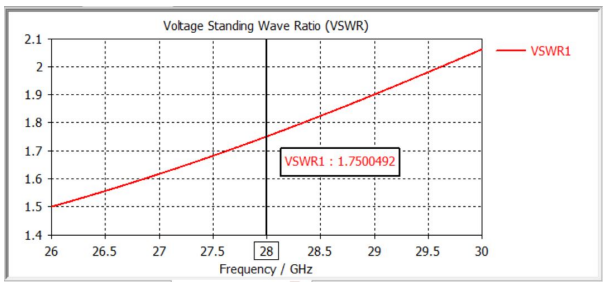

a VSWR of a mm wave single element PIFA antenna

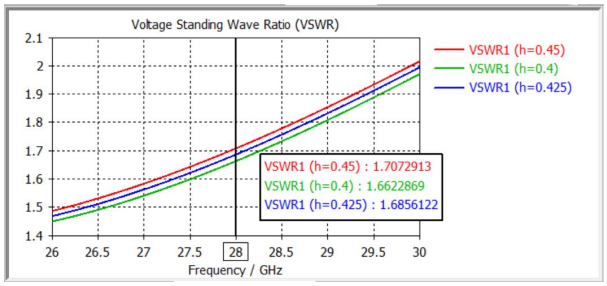

b VSWR of a h improved mm wave single element PIFA antenna

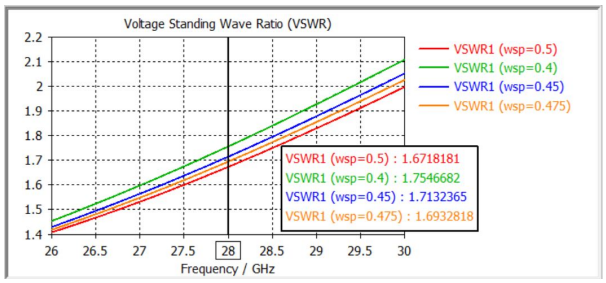

c VSWR of a ws improved mm wave single element PIFA antenna

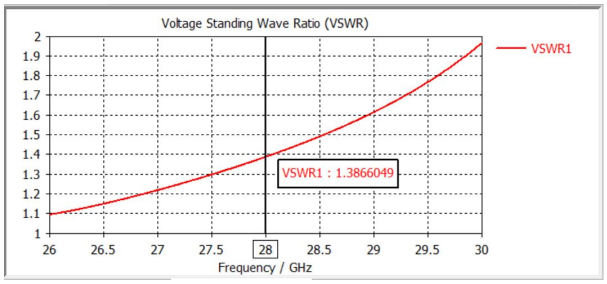

d VSWR of a slotted mm wave single element PIFA antenna

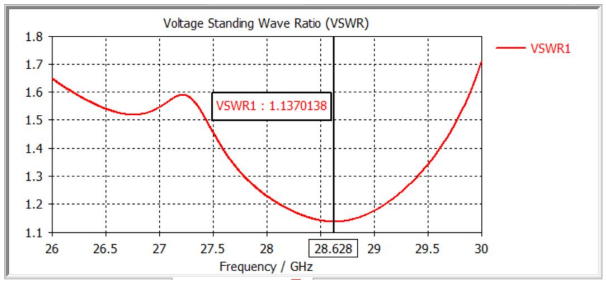

e VSWR of DGS mm wave single element PIFA antenna

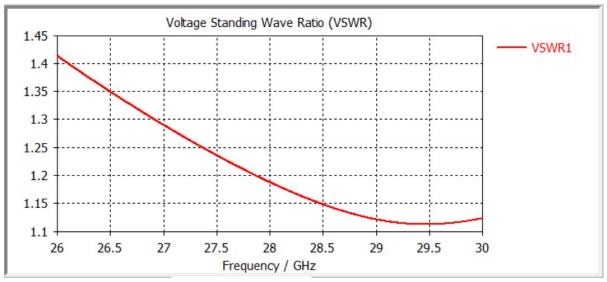

f VSWR of a parasited mm wave single element PIFA antenna

Figure 4.18: VSWR comparison of various mm-wave single element PIFA antennas

4.2.6 Current Distribution

Maximum current typically appears near the shorting pin and feed point, while weaker currents spread toward the open edges of the patch, enabling radiation in the convectional Antenna. The slots, DGS, or parasitic elements alter the current path, creating additional resonances and enhancing bandwidth by redistributing surface currents as shown in the simulation below. The DGS method achieves the best S11 -29.75dB and VSWR 1.07, indicating excellent impedance matching by creating multiple current paths that support a wider bandwidth.

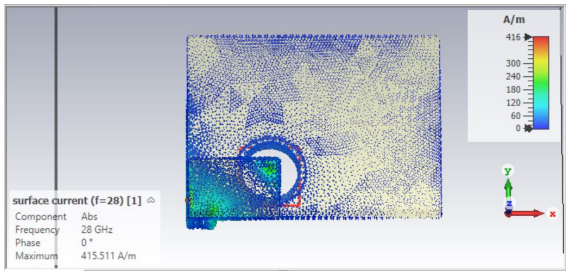

a Conventional mm-wave single-element PIFA

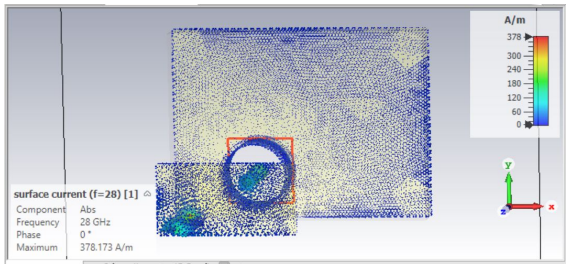

b Parasitic-loaded mm-wave single-element PIFA

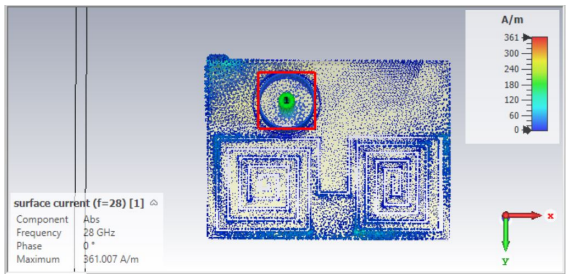

c DGS-based mm-wave single-element PIFA

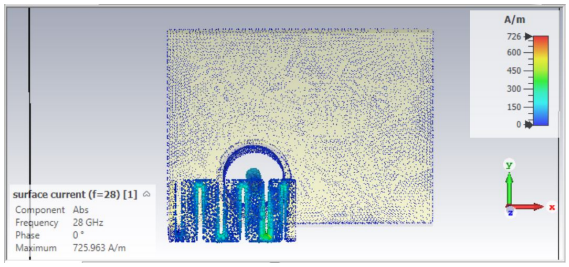

d Slotted mm-wave single-element PIFA

Figure 4.19: Surface current distribution of mm-wave single-element PIFA antennas under different loading techniques

Also, this technique yields the good gain 2.916dB by enhancing constructive radiation via mutual coupling. slot loading also offers the best performance of S11 -27dB and VSWR of 1.42, also the parasitic methode provides S11 of -25.5dB with VSWR 1.112 improving bandwidth by disrupting the ground current and suppressing surface waves. Overall, slotted, DGS and parasited techniques provide good matching which enhances the bandwidth very well.

4.3 Bandwidth

The bandwidth performance of the proposed PIFA configurations shows a clear progression as different enhancement techniques are applied. The conventional PIFA exhibits limited bandwidth with acceptable impedance matching ($S_{11} = -14$ dB) and serves as a baseline reference. The H-improved and Ws-improved designs provide moderate bandwidth enhancement, achieving dual bandwidth extensions of 423 MHz and 569 MHz, and 265 MHz and 389 MHz, respectively. Among these two configurations, the Ws-improved structure maintains the highest efficiency (76%) and the lowest VSWR, indicating better impedance stability, although the overall bandwidth improvement remains modest. Slot-loading introduces a

significant bandwidth expansion of 751 MHz, accompanied by a notable reduction in return loss (−27 dB). However, this improvement comes at the cost of reduced efficiency and gain, along with a very wide beamwidth, which may not be suitable for directive applications. The defected ground structure (DGS) technique achieves the maximum bandwidth enhancement of 841 MHz with the lowest VSWR (1.07), indicating excellent impedance matching over a wide frequency range. Although the efficiency slightly decreases, the achieved bandwidth makes the DGS configuration highly suitable for wideband 5G applications. The parasitic method provides a bandwidth comparable to DGS but with slightly reduced gain and main-lobe performance. Overall, the DGS approach offers the most balanced trade-off between bandwidth enhancement and antenna performance.

4.3.1 Performance Comparsion of BW enhancement Techniques

The bandwidth enhancement techniques applied to the mmWave PIFA antenna show distinct trade-offs in impedance bandwidth, radiation performance, and efficiency, which are critical for 5G mobile communication. The conventional PIFA exhibits limited bandwidth and moderate gain, making it unsuitable for wideband 5G applications. The improvements in height (h) and width (W_s) provide dual-band enhancement with moderate impedance bandwidth approximately 12%, but at the cost of reduced efficiency or only marginal gain improvement.

Slot loading significantly improves bandwidth to 751 MHz with a notable S_{11} of −27 dB; however, this improvement is accompanied by a reduced radiation efficiency of 64.5%and gain, which may limit the performance of the handset. Among all techniques, (DGS) demonstrates the best overall bandwidth enhancement, achieving the highest bandwidth of 841 MHz and the maximum impedance bandwidth (14.3%), along with excellent impedance matching $S_{11} = -29.75$ dB, VSWR ≈ 1.07. Although efficiency slightly decreases, the radiation characteristics remain acceptable for mobile terminals. The parasitic method also achieves a comparable bandwidth (841 MHz) and impedance bandwidth 14.3%, but shows a inferior gain and a less stable main lobe direction compared to DGS.

4.4 compare with other works

A comparative evaluation of bandwidth enhancement techniques - for millimeter-wave PIFA antennas is summarized in Table below.The EBG-enhanced design achieves a moderate bandwidth expansion of approximately 0.6 GHz and a gain of 4.05 dB with high efficiency 95.5%, but its periodic surface structure increases the fabrication complexity and the thickness of the substrate, making it less favorable for the integration of compact handsets. The AMC-backed configuration provides higher directivity, gain $\approx$ 7 dB and strong back-lobe suppression; however, the multilayer nature Of AMC surfaces introduces weight and production challenges, which restricts scalability for 5G cell terminals. PIFA designs loaded with metamaterials demonstrate useful impedance tuning and moderate bandwidth improvement 0.52GHz by incorporating resonant unit cells. Nevertheless, their design sensitivity and dependence on precise geometric parameters make them difficult to reproduce consistently at millimeter-wave frequencies. The AMC-backed approach provides the highest gain up to 5.65 dB and efficiency up to 98%, but its multi-layer configuration and alignment sensitivity make it less suitable for compact 5G smartphone designs despite modest bandwidth improvement 0.370 GHz.

In contrast, the proposed design based on the Defected Ground Structure (DGS) delivers the widest bandwidth (841 MHz) with a measured gain of 2.916dB and a radiation efficiency of 62 %, while maintaining a compact 28-GHz footprint. The introduction of precisely optimized ground-plane slots modifies surface current distribution and reduces the antenna Q-factor, thereby enhancing Impedance matching throughout a broader frequency range. This structural simplicity enables easy fabrication, stable performance, and superior compatibility with mobile-device platforms compared to complex multilayer or metamaterial configurations.Its single-layer, compact configuration makes it particularly attractive for 5G smartphone applications. In general, while AMC and metamaterial methods excel in gain improvement, the DGS approach provides the best compromise between bandwidth, efficiency, simplicity, and practical feasibility for next-generation portable devices.

Technique	**S11 (dB)**	**BW Enhanced (MHz)**	**Efficiency (%)**	**VSWR**	**Gain (dB)**	**Main Lobe =90° (dB)**	**3dB Beamwidth (°)**	**Impedance BW (%)**	**Remarks**
Conventional PIFA	-14	-	74.7	1.8	3.37	3.7	118.9	-	Baseline performance; limited bandwidth, acceptable efficiency.
H-improved	-14.6	423 & 569	68.5	1.73	3.08	3.59	119.1	12.56	Moderate bandwidth enhancement, slight efficiency drop, stable VSWR.
Ws-improved	-15.44	265 & 389	76	1.44	3.20	3.47	124.3	11.975	Small bandwidth improvement, highest efficiency, low VSWR, wider beam.
Slot-loading	-27	751	64.5	1.42	2.82	2.41	191.1	13.964	Significant bandwidth increase, moderate efficiency loss, gain slightly reduced, very wide beam.
DGS	-29.75	841	61	1.07	2.92	3.54	141.4	14.3	Maximum bandwidth achieved, low VSWR, moderate gain, slightly lower efficiency; compact design suitable for 5G.
Parasitic method	-25.5	841	61	1.112	2.69	3.24	141.7	14.3	Similar bandwidth to DGS, slightly lower gain, comparable VSWR and efficiency; effective but less optimal main lobe.

Table 4.1: Performance comparison of bandwidth enhancement techniques for mmWave PIFA antennas for 5G mobile communication.

Table 4.2: Comparison of Other Bandwidth Enhancement Techniques of PIFA Antenna

Technique	Bandwidth (GHz)	Bandwidth Enhanced (GHz)	S_{11} (dB)	Efficiency (%)	Gain (dB)	VSWR	HPBW (3dB)	Complexity / Suitability & 5G Application Comments	Authors / References
EBG-enhanced	**3.75**	**+0.67**	**-27.5**	**95.5**	**4.05**	**1.325**	**~107.5°**	**Good gain; moderate complexity due to periodic EBG elements; slightly narrower BW than DGS.**	***Kamaruddin et al., ResearchGate 2018***
AMC-backed	**3.5**	**+0.37**	**-20**	**94**	**5.65**	**1.45**	**~92.5°**	**Highest gain potential; multilayer; less practical for smartphones.**	***Kamaruddin et al., ResearchGate 2018***
Metamaterial-loaded	**3.6**	**+0.52**	**-22.5**	**94**	**3.75**	**1.3**	**~105°**	**Moderate BW improvement; complex unit-cell tuning; more difficult fabrication.**	***Hussain 2023; Nahar & Rawat 2022***
DGS (Defected Ground Structure)	**4**	**+0.841**	**-29.75**	**62**	**2.916**	**1.07**	**141.4°**	**Broad bandwidth, excellent efficiency, low complexity; ideal for compact 5G smartphones.**	**This work**

Chapter 5

5.1 Conclusions

This study evaluated several bandwidth (BW) enhancement techniques for a 28 GHz mmWave PIFA antenna designed for 5G mobile communication, including geometrical modifications (h and Ws-improvement), slot loading, defected ground structure (DGS) and parasitic element methods. The conventional PIFA exhibited a narrow bandwidth with moderate efficiency (74.7%) and a VSWR of 1.8, indicating limited suitability for wideband 5G applications. Among the techniques studied, DGS and parasitic methods achieved the highest bandwidth enhancement, reaching 841 MHz, compared to conventional PIFA. Slot loading also significantly improved bandwidth (751 MHz) while maintaining reasonable efficiency (64.5%). Geometrical modifications, such as h and Ws-improvements, provided moderate enhancements (265–569 MHz) but with a less dramatic bandwidth expansion.

From an efficiency perspective, the improved Ws PIFA achieved the highest efficiency (76%), while the DGS and parasitic techniques slightly reduced the efficiency to around 61%. Similarly, VSWR improved across all enhancement methods, with DGS showing the lowest VSWR of 1.07, indicating excellent impedance matching. Gain variations were moderate between techniques, with conventional PIFA achieving 3.37 dB and most enhanced designs remaining within 2.7–3.2 dB. Angular beam widths and main lobe directions shifted depending on the technique, highlighting a tradeoff between bandwidth, radiation pattern, and gain.

Although DGS and parasitic element methods provide the most significant bandwidth improvement, they come at the cost of slightly reduced efficiency and potential complexity in fabrication. Slot loading offers a balance between bandwidth enhancement and acceptable

radiation efficiency, although it slightly increases the beam width. Geometrical modifications are simpler to implement, but yield moderate bandwidth improvements. For maximum bandwidth enhancement in mmWave 5G PIFA applications, DGS or parasitic element techniques are the most effective, offering the highest impedance bandwidth (∼14.3%) and superior matching.

5.2 Recommendation

Combining DGS with slot or parasitic structures can maximize mmWave PIFA bandwidth for 5G, with careful design needed to balance efficiency, gain, and beam characteristics.

References

[1] R. Garg, *Microstrip antenna design handbook*. Artech house, 2001.

[2] K.-L. Wong, "Planar antennas for wireless communications." *Microwave Journal*, vol. 46, no. 10, pp. 144–145, 2003.

[3] H. A. Wheeler, "The radiansphere around a small antenna," *Proceedings of the IRE*, vol. 47, no. 8, pp. 1325–1331, 1959.

[4] Y. T. Lo and S. Lee, *Antenna Handbook: theory, applications, and design*. Springer Science & Business Media, 2013.

[5] D. Guha and Y. M. Antar, *Microstrip and printed antennas: new trends, techniques and applications*. John Wiley & Sons, 2011.

[6] H. Wu, Z. Chen, and X. Yang, "Metamaterial-loaded pifa for mmwave 5g communications," *IEEE Transactions on Antennas and Propagation*, vol. 67, no. 6, pp. 1234–1241, 2019.

[7] A. Rajaraman and J. Smith, "High dielectric constant substrates for compact antenna design," *IEEE Transactions on Antennas and Propagation*, vol. 68, no. 9, pp. 1234–1242, 2020.

[8] J. Kim and S. Park, "Enhancing pifa bandwidth with slit designs for 5g mmwave communication," *IEEE Transactions on Antennas and Propagation*, vol. 69, no. 10, pp. 1234–1245, 2021.

[9] X. Li and L. Zhao, "Stacked radiating elements in pifa for wideband 5g applications," *Microwave and Optical Technology Letters*, vol. 64, no. 2, pp. 567–573, 2022.

[10] Z. Qi, X. Ding, W. Yang, and J. Chen, "A compact broadband planar inverted-f antenna with dual-resonant modes," *Applied Sciences*, vol. 12, no. 17, 2022.

[11] N. Liu, L. Zhu, and W. Choi, "A low-profile wide-bandwidth planar inverted-f antenna under dual resonances: Principle and design approach," *IEEE Transactions on Antennas and Propagation*, vol. 65, pp. 5019–5025, 2017.

[12] H. T. Chattha, Y. Huang, and Y. Lu, "Pifa bandwidth enhancement by changing the widths of feed and shorting plates," *IEEE Antennas and Wireless Propagation Letters*, vol. 8, pp. 637–640, 2009.

[13] Y. Lu and M. M. Tentzeris, "A reconfigurable microstrip-fed pifa for mm-wave 5g applications." *IEEE Transactions on Antennas and Propagation*, vol. 66(10), pp. 5012–5016, (2018).

[14] P. Deshmukh and M. D. Desmond, "Performance enhancement of a microstrip-fed pifa antenna for 5g base stations." *IEEE Wireless Communications Letters*, vol. 8(5), pp. 1389–1392, (2019).

[15] P. Kumar, T. Ali, O. P. Kumar, S. Vincent, P. Kumar, Y. Nanjappa, and S. Pathan, "An ultra-compact 28 ghz arc-shaped millimeter-wave antenna for 5g application," *Micromachines*, vol. 14, no. 1, p. 5, 2023. [Online]. Available: https://doi.org/10.3390/mi14010005

[16] W. Ahmad and W. T. Khan, "Small form factor dual band (28/38 ghz) pifa antenna for 5g applications," in *2017 IEEE MTT-S International Conference on Microwaves for Intelligent Mobility (ICMIM)*, 2017, pp. 21–24.

[17] G. K. Soni, D. Yadav, A. Kumar, P. Jain, and M. V. Yadav, "Design and optimization of flexible dgs-based microstrip antenna for wearable devices in the sub-6 ghz range using the nelder-mead simplex algorithm," *Results in Engineering*, vol. 24, p. 103470, 2024.

[18] T. Nahar and S. Rawat, "Survey of various bandwidth enhancement techniques used for 5g antennas," *International Journal of Microwave and Wireless Technologies*, vol. 14, no. 2, pp. 204–224, 2022.

[19] R. Kamaruddin, I. Ibrahim, N. Nor, S. Yusoff, Z. Zakaria, N. Shairi, M. Abu, and T. Rahman, "A study on the ebg and amc on radial line slot array structure at 28 ghz," *Journal of Telecommunication, Electronic and Computer Engineering (JTEC)*, vol. 10, no. 2-6, pp. 129–134, 2018.

[20] P. W. Chan, H. Wong, and E. K. N. Yung, "Wideband planar inverted-f antenna with meandering shorting strip," *Electronics Letters*, vol. 44, no. 6, pp. 395–396, Mar. 2008.

[21] R. Feick, H. Carrasco, M. Olmos, and H. D. Hristov, "Pifa input bandwidth enhancement by changing feed plate silhouette," *Electronics Letters*, vol. 40, no. 15, pp. 921–922, Jul. 2004.

[22] C. A. Balanis, "Antenna theory, hoboken." *New Jersey: John Wiley & Sons*, vol. 8, p. 21–31, (2005).

[23] K. P. Simon, "Foundations of antenna engineering : A unified approach for line-ofsight and multipath." *Chalmers University of Technology*, (2017).

[24] M. Newell, E. Tuley, H. G. Gillespie, E. Oltman, E. Urbanik, A. D. Hart, A. Olver, D. F. Villeneuve, Reilly, I. N. Franklin, R. H. Knight, R. Reimer, J. L. García, and Koepfinger, "Ieee standard definitions of terms for antennas," *IEEE Transactions on Antennas and Propagation*, pp. 145–1993, (1993).

[25] S. N. Makarov, "Antenna and em modeling with matlab," *Journal Name*, 2002.

[26] N. Chavda, D. Vedvyas, and P. Kiran, "Designing of microstrip patch antenna for 3g-wcdma applications," *International Advanced Research Journal in Science, Engineering and Technology*, vol. 1, p. 49–53, (2012).

[27] A. F. Alsager, "Design and analysis of microstrip patch antenna arrays," *Unknown Journal*, (2011).

[28] Antenna-Theory.com. (2009-2021) Planar inverted-f antenna (pifa). https://www.antenna-theory.com/antennas/patches/pifa.php.

[29] A. Kumar, J. Kaur, and R. Singh, "Performance analysis of different feeding techniques," *International journal of emerging technology and advanced engineering*, vol. 3, no. 3, pp. 884–890, 2013.

[30] G. Kumar and K. P. Ray, *Broadband microstrip antennas*. Artech house, 2003.

[31] A. A. Omar, M. A. Abdalla, and H. H. Abdullah, "Bandwidth enhancement of millimeter-wave pifa using parasitic elements," *IEEE Transactions on Antennas and Propagation*, vol. 68, no. 7, pp. 4954–4962, July 2020.

[32] C. A. Balanis, *Antenna Theory: Analysis and Design*, 4th ed. Wiley, 2016.

[33] D. M. Pozar, *Microwave Engineering*, 4th ed. Wiley, 2012.

[34] E. Hammerstad and O. Jensen, "Accurate models for microstrip computer-aided design," *IEEE MTT-S Int. Microwave Symp. Digest*, pp. 407–409, 1980.

[35] M. Tayel, T. Abouelnaga, and A. Elnagar, "Pencil beam grid antenna array for hyperthermia breast cancer treatment system," *Circuits and Systems*, vol. 8, no. 5, May 2017.

[36] A. Rachmansyah and A. Mutiara, "Designing and manufacturing microstrip antenna for wireless communication at 2.4 ghz," *International Journal of Computer and Electrical Engineering*, vol. 3, no. 5, pp. 670–675, 2011.

[37] J. M. Rathod, "Design development of antenna for tvtransmission for connecting outdoor broadcastsvan to the studio for rural areas," *International Journal of Computer and Electrical Engineering*, vol. 2, no. 2, p. 251, 2010.

[38] S. Maiti, S. Rajak, and A. Mukherjee, "Design of a compact ultra wide band microstrip patch antenna," in *Computing, Communication and Networking Technologies (ICCCNT), International Conference on.* IEEE, 2014, pp. 1–3.